UNIVERSITY OF MINNESOTA

ST. ANTHONY FALLS LABORATORY
Engineering, Environmental and Geophysical Fluid Dynamics

Project Report No. 590

Transport of Chloride through Silt Loam, Sandy Loam and Sandy Loam with Compost

Final Report for the Project:
Impacts of Adding Salt to Our Minnesota Lakes, Rivers, and Groundwater

by

Andrew J. Erickson, John S. Gulliver, and Peter T. Weiss

St. Anthony Falls Laboratory, University of Minnesota,
2 Third Avenue SE Minneapolis, MN 55455

Prepared for
Legislative-Citizen Commission on Minnesota Resources

December 2019
Minneapolis, Minnesota

ACKNOWLEDGEMENTS

Funding for this project was provided by the Minnesota Environment and Natural Resources Trust Fund as recommended by the Legislative-Citizen Commission on Minnesota Resources (LCCMR). he Trust Fund is a permanent fund constitutionally established by the citizens of Minnesota to assist in the protection, conservation, preservation, and enhancement of the state's air, water, land, fish, wildlife, and other natural resources. Currently 40% of net Minnesota State Lottery proceeds are dedicated to growing the Trust Fund and ensuring future benefits for Minnesota's environment and natural resources. For more information about the LCCMR, visit https://www.lccmr.leg.mn/index.html

The project, "Impacts of Adding Salt to Our Minnesota Lakes, Rivers, and Groundwater," as funded under Legal Citation: M.L. 2016, Chp. 186, Sec. 2, Subd. 04n was a collaborative effort between the authors of this report and other investigators and project partners. The authors wish to thank Co-principal investigator Sara Heger (University of Minnesota Water Resource Center and Department of Bioproducts and Biosystems Engineering) and Alycia Overbo for their diligence and effort on Activities 1 and 2 of this project. In addition, the authors are thankful to Andrew Ronchak and Brooke Asleson from the Minnesota Pollution Control Agency for contributed in-kind match in the form of support, communication, and collaboration on this project. Finally, the authors wish to thank Connie Fortin, Carolyn Dindorff, and other staff at Fortin Consulting for their contributions to this project.

Support and assistance were provided by staff and students at St. Anthony Falls Laboratory and is greatly appreciated, including Jenni Larson, Lisa Ostland, Chris Milliren, Rob Gabrielson, Peter Corkery, Camila Merino Franco, Parker Brown, Anna Healy, and Nam Nguyen.

EXECUTIVE SUMMARY

The purpose of this project was to measure the transport of chloride from road salt through soils commonly found in Minnesota. Previous research in Minnesota and other areas have shown that chloride does not move freely with water but interacts with soil in unexplained ways. The result is periods of chloride capture by soil and other periods of chloride release, which impacts chloride transport and loading to surface and groundwater resources.

This project used column experiments to illustrate chloride movement through silt loam, sandy loam, and sandy loam with 10% organic material, which are common in Minnesota. The column experiments corroborated observations in the literature that chloride is sometimes stored within the soil and released slowly at later times. The data, however, did not provide insight into the processes involved.

Field cores were also collected during summer at two sites targeting silt loam and sandy loam, though texture analysis revealed that the cores were primarily sandy clay loam with portions of silt loam and sandy loam. At each site, cores were collected in the drainage ditch at four locations: near the road, mid-slope, at the bottom of the drainage ditch and mid-slope on the far side. The chloride content was the highest near the road, between 1.5 and 3 meters in depth, indicating that the content had been washed down by summer rain storms infiltrating into the soil. Chloride content was relatively high throughout the soil core depth in the center of each channel, indicating a long-term exposure to road salt. The chloride content was lowest on the far slope, away from the road. The results of the field cores demonstrate that chloride is present in the soil along roadways that are treated with deicing road salt.

It is not clear from the column experiments or field cores which soil or hydraulic properties cause capture or release of chloride from road salt. The data demonstrate that there are complex transport and exchange processes affecting chloride within the soils which simple physical processes cannot explain.

The observations for these experiments and field data indicate that chloride management in Minnesota has complex and (currently) unpredictable ramifications to Minnesota's water resources. Simple assumptions are not appropriate, and more research is needed to understand the long-term impacts of decisions made about chloride management.

TABLE OF CONTENTS

FIGURES

TABLES

CHAPTER 1: INTRODUCTION

This report is part of the Environment and Natural Resources Trust Fund (ENRTF) funded project titled *Understanding Impacts of Salt Usage on Minnesota Lakes, Rivers, and Groundwater*. This report satisfies, in part, Activity 3 of the project, which is "Chloride transport through, and retention in, Minnesota soils." Activity 1 (Estimate statewide sodium chloride use) and Activity 2 (Develop best management practices to reduce salt due to water softening) are outside the scope of this report.

In the State of Minnesota, the amount of salt (sodium chloride) used to de-ice roads, parking lots, and sidewalks increased by 230% between 1991 and 2006 (Novotny, Murphy, & Stefan, 2008). The amount of salt used for road deicing is enormous. For example, a recent average of 174,000 tons of road salt is applied to just those roads maintained by MnDOT each year (MnDOT, 2019) and over 349,000 tons of road salt were found to be applied to roads in the Twin Cities Metro Area each year (Novotny et al., 2008). Additional salt is applied to other county and municipal roads each winter for deicing purposes. Road deicing salt infiltrates into roadside soils during snowmelt events or directly runs off into surface waters. The sodium is trapped by the soil and other particles and can inhibit vegetation growth in affected soils. Chloride will move through the soil to receiving water bodies or groundwater, resulting in an impact on the aquatic biota of these waters, as seen by the roughly 50 impairments for chloride in Minnesota (MPCA, 2019).

Previous research has shown that de-icing salt is the dominant source of chloride in the Twin Cities metro area and is accumulating to toxic levels in many lakes, wetlands and rivers (Novotny et al., 2008). There are many unknowns, however, with regards to the accumulation and transport of chloride in the soil and groundwater. Historically, it was typically assumed that chloride is conservative, meaning that it follows fluid particles and does not interact in the environment and, therefore, can be totally recovered. The research herein will show that this is not necessarily true. The transport of chloride in a soil and/or groundwater system may lag and chloride may be stored in the media and released later. There may be interactions with microorganisms and chlorides may be bound, from temporarily to semi-permanently, with organic matter. Thus, it is not fully known how or where chloride is being stored in Minnesota soils. The ultimate fate or destination of the chloride and any corresponding travel times are also not fully known. A better understanding of the processes and mechanisms of chloride transport and storage in soil and groundwater is imperative in order to answer critical questions such as the extent and timing of any impact of chloride on drinking water sources in the state or how changes in chloride loading to the environment will impact concentrations in surface and groundwaters.

Activity 3 of this project seeks to answer these questions through analysis of soil samples and column studies to investigate the transport of chloride through the soils. The objective is to enhance an existing chloride transport model by incorporating chloride residence time as a function of soil properties. The transport model will then be able to better predict the response of chloride transport into surface water and groundwater as a result of reductions in salt loading.

CHAPTER 2: LITERATURE REVIEW

Most of the research to date on the interaction and transport of chloride through soil was related to salt water intrusion and its interaction from the ocean. Early studies compared exchange rates for chloride and other ions while later studies have considered reactions with natural organic matter and vegetation-mediated impacts to chloride movement. The most important source of chloride to coastal forest ecosystems is sea salt deposition, though volcanoes and coal burning can also be important sources and de-icing and anti-icing salt can be an important chloride input near major roads (Clarke et al., 2009). As a result, chlorine is present as chloride ion and/or chlorinated organic matter in temperate and boreal forest ecosystems and it contributes to the degradation of soil organic matter, thus also affecting carbon sequestration in the forest soil (Clarke et al., 2009).

2.1 ANION EXCHANGE

Anion exchange competition between chloride, nitrate, sulfate, and phosphate was investigated for three soils that have high contents of amorphous inorganic materials (Kinjo & Pratt, 1971). The soils had slightly more affinity and capacity for chloride compared to nitrate. It is hypothesized that the adsorption mechanism for chloride and nitrate is the same for these soils and that chloride replaces more hydroxyl ions (OH^-) compared to nitrate (Kinjo & Pratt, 1971). This indicates that chloride, when exposed to soils, may adsorb and be retained by the soil surface.

2.2 INTERACTIONS WITH ORGANIC MATTER

Natural organochlorine production appears to be associated with the decomposition of plant material on the soil surface, though the chlorine cycle budget implies that a proportion of natural organochlorine enters soil through plant litter and atmospheric deposition as well (Leri & Myneni, 2010). Organochlorine compounds may form through biotic and abiotic pathways, but the rates and magnitude of production in the field remain undefined. It is hypothesized that multiple pools of chlorinated organic matter exist in the soil environment and that leaf litter deposition makes a significant and refractory contribution to the soil organochlorine pool.

In-situ X-ray spectroscopy indicated that natural organic matter in soils, sediment, and natural waters contain stable compounds with chlorinated phenolic and aliphatic groups as the main chlorine form (Myneni, 2002). Compounds are formed rapidly from inorganic chlorine during plant matter humification. The concentration of aromatic organochlorine in decaying plant litter varies seasonally but exhibits a cumulative increase with decay time. This leads to the enrichment of chloride in surface soil in the form of chlorinated organic matter. The soil column displays a change in chloride speciation from organic to inorganic with depth, which may be attributable to biodegradation and/or abiotic transformations.

Halogen (chlorine, bromine, and iodine) retention in peat was investigated in two peat bogs in southernmost Chile (Biester, Keppler, Putschew, Martinez-Cortizas, & Petri, 2004). Natural atmospheric wet deposition of chlorine to these peat bogs ranges from 600 – 36000 mg per m^2 per year. Accumulation rates for chlorine was calculated to be 12 – 72 per m^2 per year, suggesting a retention rate of (0.2-2%). This is significantly less than retention rates for bromine (7.5 – 50%) and iodine (36 – 46%) (Biester et al., 2004). Of the chlorine found in the peat, 95% was organic-bound.

Column experiments on undisturbed soil cores from a coniferous forest in Sweden were used to understand cycling of chloride to organic matter (Oberg & Sanden, 2005). The columns were irrigated with artificial rain and the runoff and leachate were collected and analyzed. The concentrations of chlorinated organics and chloride were much greater in the leachate compared to the runoff. Approximately 20 – 50% of the chloride leached from the soil was organic-bound, and the amount remained consistent throughout the experiment. The authors hypothesized that the topsoil contained significant amounts of chlorinated organics that were leaching to deeper soil layers and that organic matter precipitates or is mineralized as chloride moves through the soil (Oberg & Sanden, 2005).

Lysimeters were installed in soil from a coniferous forest in southeast Sweden to determine if pore water residence times and chloride load affected chloride retention (D. Bastviken et al., 2006). During the experiments, chloride was initially captured by the soil but subsequently released. Retention and subsequent release rates increased with increased soil-water residence time and increased chloride loading rate. The authors hypothesized that chloride retention was due to chlorination of the soil organic matter or ion exchange, though ion exchange didn't appear to be significant, and that the shift from chloride retention to release is due to the presence or lack of oxygen or microbially-available organic matter.

Undisturbed soil columns collected from a coniferous forest in southeast Sweden were investigated to determine impacts of time, temperature, oxic/anoxic conditions, and depth of soil on chloride retention (David Bastviken, Svensson, Karlsson, Sandén, & Öberg, 2009; D. Bastviken et al., 2007). The soil water content was approximately 33% and dry weight of organic matter was approximately 27%. Initial total organic chlorine content of the soil was approximately 133 µg/g dry weight and the extractable inorganic chlorine was approximately 21 µg/g dry weight. Chloride retention in this soil between 4 °C and 40 °C was biotic and driven by oxygen-dependent enzymes, with the most retention occurring at optimal temperatures for the microbes (20 °C). Minimum chloride retention rates were observed at high temperatures (e.g., 50 °C) or under anoxic conditions.

A chlorine isotope (^{36}Cl) tracer was used to study chlorination rates with organic matter in eleven different locations including coniferous forest soils, pasture soils and agricultural soils (Gustavsson et al., 2012). Chlorination rates were largest in the forest soils and strong correlations between chlorination rate and soil organic matter content or chloride concentration were identified. In addition, soils with more organic matter were linked with more organic-bound chlorine and greater supply of chloride that is susceptible to de-chlorination and subsequent release (Gustavsson et al., 2012). (Johansson, Sanden, & Oberg, 2003) found that the concentration of organically bound chlorine was positively correlated to the organic carbon content. The spatial distribution patterns, however, strongly indicate that some other variable adds structure to the spatial distribution of organic chlorine.

Results from a long-term reforestation experiment (Montelius et al., 2015) showed that the abundance and residence times of chlorine and organochloride after 30 years were highly dependent on which tree species were planted on the nearby plots. Average chlorine and organochlorine content in soil humus were higher at experimental plots with coniferous trees than in those with deciduous trees. Plots with Norway spruce had the highest net accumulation of chlorine and organochlorine over the experiment period and showed 10 and 4 times higher chlorine and organochlorine storage (kg ha−1) in the biomass, respectively, and 7 and 9 times higher storage of chlorine and organochlorine in the soil humus layer, compared to plots with oak. The results can explain why local soil chlorine levels are frequently independent of atmospheric deposition and provide opportunities for improved modeling of chlorine distribution and cycling in terrestrial ecosystems.

From field observations of organic carbon, chloride, and chlorinated organic carbon (Svensson, Sanden, Bastviken, & Oberg, 2007) concluded that 1) The soil pool is dominated by chlorinated organic carbon, 2) The input via wet deposition of chloride and output of chloride in runoff is 30 times smaller than the total storage of chloride and chlorinated organic carbon in soil, and 3) transport is dominated by chloride. It was also stated that organic matter that "entered the outlet" (presumably meaning to leave the study area) was more chlorinated in fall than the rest of year.

2.3 UNSATURATED FLOW

Unsaturated flow is complicated by the three forms of media present, liquid (water), gas (air) and solid (soil matrix). Artificial rainfall was applied at a near-constant rate to two soil types and chloride breakthrough was measured under unsaturated flow conditions (Bejat, Perfect, Quisenberry, Coyne, & Haszler, 2000). Experiment data was fit to the convection dispersion equation with estimated values for pore water velocity, dispersion coefficient, and (for some) maximum bulk electroconductivity. Increasing water content resulted in decreasing pore water velocity and decreasing dispersion coefficient. The authors concluded that solute dispersion in unsaturated soils under similar conditions are likely related to differences in water content at a given flow rate produced by differences in pore size distribution (Bejat et al., 2000).

The structure of an unsaturated soil zone was investigated to assess the groundwater vulnerability of salt contamination (Fetisova, Fetisov, De Maio, & Zektser, 2016). Results indicated that the main parameters that define travel time of chlorides through the unsaturated zone to the groundwater are seepage velocity of the infiltrating flow and the hydraulic conductivity of the unsaturated zone.

A 2-dimensional solute model was used to investigate the mechanisms controlling chloride transport and the unsaturated zones ability to act as a reservoir (Lax & Peterson, 2009). Simulations showed that within the unsaturated zone chloride transport is mostly vertical and driven by molecular diffusion. Chloride was retained in the saturated zone with a net loss of Cl in the unsaturated zone for the first 10 years of simulation. In year 11 a steady state between chloride input and output was achieved. Ultimately, chloride in the unsaturated zone became a long-term source of chloride to groundwater.

The influence of NaCl on the contact angle between NaCl solution, air, and various surfaces was demonstrated by (Sghaier, Prat, & Ben Nasrallah, 2006). The NaCl caused the contact angle to increase significantly on all hydrophilic surfaces. It was noted that contact angle changes may have a major effect on salt transport and evaporation in unsaturated soils or porous materials due to a possible change in the hydraulic connectivity associated with thick films.

2.4 CRYSTALLIZATION, EVAPORATION, AND PRECIPITATION

Salt crystallization can extend above saline water table, travelling up non-porous surfaces through wicking (Hazlehurst, Martin, & Brewer, 1936; Washburn, 1927). Evaporation causes the brine solution to be supersaturated, which causes nucleation of crystals at the brine surface meniscus. More crystals develop from the solute films that bind the crystals, which releases water vapor and process is repeated. This leads to the formation of dendrite of crystallization. The result is a fine-grained microporous structure that enhances movement through capillary action, which advances the crystal front in the fashion of a wick.

X-ray was used to investigate salt precipitation due to evaporation and the effects of particle and pore sizes on the precipitation pattern (Norouzi Rad & Shokri, 2015). Results showed the presence of preferential evaporation sites (associated with fine pores) on the surface of sand columns significantly influences the patterns and dynamics of NaCl precipitation. There is the formation of thicker salt crust with thicker grain size on the surface with fewer fine pores. Fewer fine pores on the surface also resulted in shorter stage-1 precipitation for columns with larger grain sizes.

A three-year study in northwest China investigated the distribution of salt accumulation in soils subjected to under-mulch drip irrigation (Zhang et al., 2014). The particle size distribution of the soil had a significant impact on salt migration and distribution; salt accumulates along impermeable layers such as when the soil changes rapidly from sand to clay. In addition, the distribution of dissolved salts in the soil profile follows the pattern of water flux and there's a tendency for salts to accumulate at the periphery of the wetted soil. In the root zone (cotton plants) there is an exponential relationship between soil electroconductivity (EC, i.e., salts) and clay/silt particle content. In sandy soil, salt did not accumulate in the root zone or the deep zone because the salt was leached due to high permeability of the sandy soil (Zhang et al., 2014).

2.5 WATERSHED MEASUREMENT AND MODELING

Long-term sodium chloride retention was investigated in a rural watershed in SE New York State (Kelly et al., 2008). Sodium and chloride concentrations and export increased from 1986 to 2005 in a rural stream. Concentrations increased by 1.5 mg/L and 0.9 mg/L per year for chloride and sodium, respectfully. Export also increased 33,000 kg/yr for chloride. Road deicing salt was estimated to account for 91% of the NaCl input load. Model results suggested that the increase in concentration and export was due to release/lag effect of long-term use of salt and subsurface build up.

A separate study investigated the potential of groundwater and soils to act as reservoirs of chloride in a watershed of a small, rural stream in New York State (Kincaid & Findlay, 2009). In this study soil cores were irrigated in the lab with sodium chloride solution followed by a chloride-free solution. During sodium chloride dosing chloride concentrations in core leachates were less than influent indicating some retention. After chloride-free water was dosed on the columns, leachate concentrations declined but did not reach stormwater concentrations until the equivalent of 15 cm of precipitation was added to the column. It was concluded that soil retention and gradual release may act as a temporary reservoir and source of chloride, thereby linking wintertime salt applications with summer surface water concentrations.

Chloride budgets were compiled from 32 catchment studies to determine the extent to which chloride is conserved in passage through a forest ecosystem (Svensson, Lovett, & Likens, 2012). Sites ranged from having net output to net input. Sites with low chloride deposition consistently showed a net release of chloride, suggesting an internal source or a declining internal pool. Chloride may be conservative in sites with a high chloride deposition but might not be in sites with low deposition.

Other studies typically attribute chloride imbalances to unmeasured atmospheric deposition, mineral weathering, and interactions with vegetation and soil. But recent studies indicate chloride participates in a complex biogeochemical cycle (Svensson et al., 2012). Chloride can be immobilized in ecosystems by 1) ion exchange, 2) adsorption on to iron and aluminum oxides, and 3) uptake by biota including vegetation and microbes. These processes can act as a source or a sink in the ecosystem.

A chlorine budget on a watershed in Sweden was performed (Oberg, Holm, Sanden, Svensson, & Parikka, 2005). The principal input and output fluxes of chlorine in the catchment are inorganic but that the main pool is organic-matter-bound chlorine in the soil. Calculations suggest that a considerable portion of chloride in soil is transformed to organic-matter-bound chlorine and leached to deeper soil layers, that net mineralization of organic-matter-bound chlorine takes place in soil, preferably in deeper soil layers, and that degrading organic matter is a major source of chloride in runoff. Dry deposition of chloride is at risk of being underestimated if chloride is assumed to be conservative in soil. The pool of organic-matter-bound chlorine in soil is considerably larger than the annual flux of chloride through the system. The estimates suggest that the amount of organic-matter-bound chlorine in the upper 40 cm of the soil at the investigated site is approximately twice as large as the chloride. Furthermore, the amount of organic-matter-bound chlorine biomass is small in relation to the occurrence of organic-matter-bound chlorine in soil. Finally, the estimates indicate that the transport of volatile organic-matter-bound chlorine from the soil to the atmosphere may influence the chlorine cycle.

Surface water and groundwater samples collected in and around an urban stream near a major highway exhibited impacts from road salt used on the highway (Cooper, Mayer, & Faulkner, 2014). Samples collected in a nearby stream that is not near a major highway did not exhibit similar salt impacts. In addition, samples collected through the year suggested that salt was accumulating in and exporting from shallow groundwater.

Chloride leaching in a large watershed from diffuse and point sources was quantified from 1900 to 2010 with the intent to determine impact of land use and management practices (Kopacek, Hejzlar, Porcal, & Posch, 2014). Over that time frame major watershed changes were that chloride input from fertilizers and livestock, and atmospheric deposition tripled in the 1950s through the 1980s and then suddenly decreased and the fraction of drained land rapidly increased from 4% in 1950 to a maximum of 43% in the 1990s.

An integrated catchment model for salinity was used to assess the transport of road salt from in watersheds to streams using landscape, hydrologic, and meteorological and salt application data (Jin, Whitehead, Siegel, & Findlay, 2011). Results suggested that a dominant mode of catchment simulation that does not entail complex deterministic modeling is an appropriate method to model salinization and assess effects of future applications of road salt to streams. The model was a dynamic mass balance model and attempted to track temporal variations in hydrological flow paths, transformations and stores, in both the land and stream components. Two model runs assuming that 1) all households and 2) half of households had water softeners showed resulting chloride concentrations differing by only 6.2 +/- 3.3%. Model results generally were close to measured values except observed concentrations were dampened and didn't have some fluctuations predicted by the model. It was stated that there could be an attenuation process in the watershed that was not incorporated into the model.

2.6 CHLORIDE IN STORMWATER TREATMENT PRACTICES

Chloride fate and transport was modeled for a constructed wetland that receives a large chloride concentration from wastewater effluent (Hu et al., 2013). Advective transport in the surface water (71%) and through groundwater (24%) accounted for most of the chloride. Approximately 5% volatilized into air and was blown out of the study area by wind and 0.08% was transported by harvest and death of reed vegetation.

2.7 CHLORIDE INTERACTION WITH MICROORGANSIMS

Chloride concentration affects the indigenous microbial community in experimental soil (Gryndler, Rohlenova, Kopecky, & Matucha, 2008). This was documented on an unidentified microorganism whose DNA was detectable in soil high in chloride but was not found in soil with low chloride concentration. The presence of the organism responsive to increased chloride concentration was associated with the highest observed value of chlorination of humic acid, suggesting a possible role of this organism in soil chlorine turnover. High chloride concentration in the soil tended to decrease the rate of degradation of trichloroacetic acid.

There is evidence that organohalide-respiring *Chloroflexi* (i.e., Chlorobacteria) are widely distributed as part of uncontaminated terrestrial ecosystems, they are correlated with the fraction of total organic carbon (TOC) present as organochlorines, and they increase in abundance while dechlorinating organochlorines. Findings suggest that organohalide-respiring *Chloroflexi* may play an integral role in the biogeochemical chlorine cycle (Krzmarzick et al., 2012).

Sediment grab samples and cores were taken to explore whether a sulfur gradient impacted organohalide-respiring *Chloroflexi* in lake sediments (Krzmarzick, McNamara, Crary, & Novak, 2013). They increased in number from west to east, whereas lake sulfate concentrations decreased along the west-to-east transect. Statistical analyses showed that dissolved sulfur in the pore-water, measured as sulfate after oxidation, appeared to have a negative impact on the total number of putative organohalide-respiring Chloroflexi, the number of *Dehalococcoidetes* terminal restriction fragments (TRF), and the percentage of the terminal restriction fragment length polymorphism (TRFLP) amplification made up by *Dehalococcoidetes*. These findings point to dissolved sulfur, presumably present as reduced sulfur species, as a potentially controlling factor in the natural cycling of chlorine, and perhaps as a result, the natural cycling of some carbon as well.

CHAPTER 3: METHODS AND MATERIALS

3.1 COLUMN EXPERIMENTS

Column studies were performed on three types of soil common in Minnesota (Heitkamp & Marr, 2015): silt loam, sandy loam, and sandy loam with organics. Soils were acquired from a local aggregate supplier (Plaisted Companies, Inc. https://plaistedcompanies.com/) and mixed to create specific soil types: silt loam (20% Sand, 65% Silt, 15% Clay), sandy loam (65% Sand, 25% Silt, 10% Clay), and sandy loam with 10% organic by volume (~3% by weight). Five replicates for each of the three soil types were fabricated in fifteen vertical, wall-mounted, columns which were constructed from clear acrylic pipe and standard PVC connectors and glued together according to manufacturer's recommendations. In each column, approximately 5 cm of coarse (~1 cm diameter) beads was added to the bottom of the column, then approximately 3 cm of medium (~ 0.6cm diameter) glass beads was added, then approximately 25 cm of one of the aforementioned soils, and finally 3 cm of coarse beads were added to the top of each column (i.e. on the soil surface). The beads on the bottom were added to minimize soil particles being washed out of the column and the beads on the top of the soil were added to minimize disturbance of the surface soil when water was added to the column.

The soil was added to each column as dry material and consolidated by gently tapping the side of each column while soil was added. The average porosity for each soil type was 40% (silt loam), 35% (sandy loam), and 34% (sandy loam w/ organic). A valve was added to the bottom of each column to stop flow when desired. A spout below the valve on each column allowed water to be drained into a clear acrylic block that was machined to pass water through the opening of an electrical conductance probe (Sensorex 10k NTC Thermistor, Part Number 170354) and outflow into a tipping bucket pulse counter mechanism. The electrical conductance probes measured electrical conductance and water temperature which were calibrated using standard solutions of NaCl within the acrylic block. The tipping bucket pulse counter was measured for accuracy using standard graduated cylinders to measure volume (4.12 – 5.05 mL) per tip. The electrical conductance probes and tipping bucket mechanisms were wired to two Campbell Scientific CR1000 data loggers to record measurements every one minute.

Each column represents ~25 cm of soil depth which would be flushed by approximately one pore volume under plug-flow conditions. For reference, one pore volume is ~ 7 mL per cm^2 for the silt loam columns, ~ 7.2 mL per cm^2 sandy loam columns, and ~ 7.6 mL per cm^2 for the sandy loam with 10% organic columns. Assuming an average annual rainfall of approximately 76 cm and that 1.4% of precipitation percolates into groundwater (Albright et al., 2004), approximately 1 cm (~1 mL per cm^2) of water depth will percolate into Minnesota soils per year. Thus, each column has capacity to store approximately 7 - 8 years' worth of Minnesota precipitation.

Phases of salt-laden and salt-free runoff were added to the columns via gravity with approximately 3 m of pressure from a supply reservoir. Phases of salt-laden water were designed to represent periods of snowmelt in which road salt-laden water infiltrates into the soil and percolates through to shallow and deep groundwater. The salt-free rinse portion of each phase was designed to represent relatively salt-free rain infiltrating into the soil. The length of the salt-laden and salt-free rinse portions were determined when each column approached a steady-state concentration, and thus varied between columns and phases.

The reservoir consisted of a large (~105 L) fully-mixed tank and smaller (~4 L) constant-head tank. Within the smaller tank, a horizontal weir allowed water to flow from the smaller tank back into the larger tank. A valve-controlled connection within the reservoir of the smaller tank (i.e., upstream of the horizontal weir) allowed water to pass from the smaller constant-head tank to a manifold which distributed the water to the fifteen columns. A submerged pump within the large tank pushed water into the smaller tank and then over the horizontal weir. The crest of the horizontal weir maintained a near-constant water surface elevation because the flow rate of the columns was much less than the flow capacity of the pump. An electrical conductance and temperature probe within the constant-head tank recorded conductivity and temperature.

Prior to the initial experiment, the soil columns were filled with water from the bottom of each column to allow air to escape from the top of the soil profile and thus minimize trapped air pockets within the soil. During experiments the flow in each column was gravity-driven and thus varied for each column. In addition, the addition of salt changed the saturated hydraulic conductivity in each column by different amounts. Between experiments, the water was drained from all the column until the water surface was near the soil surface, thus maintaining saturated conditions.

Salt-laden runoff was mixed to a target concentration of approximately 1000 mg/L to represent snow-melt. Readily available food-grade NaCl (i.e., table salt) was used to dose the water in the supply reservoir and create the salt standards used to calibrate the electrical conductivity probes. Reservoir water was mixed using potable water and the salt standards were mixed using ultrapure water (Milli-Q, 18.2 MΩ-cm). Conductivity was temperature-corrected to a standard temperature of 25 °C using Equation 1 (aqion, 2019). For salt-free runoff, the reservoir was rinsed thoroughly and filled with potable water (no salt) with a background chloride concentration of 55-68 mg/L.

$$EC_{25\,°C} = EC / [\,1 + a\,(T - 25)\,] \qquad \text{with} \quad a = 0.020 \qquad (1)$$

where:
EC = Electrical Conductance at temperature, T
$EC_{25\,°C}$ = Electrical Conductance at 25 °C
T = Temperature (°C)

The electrical conductance probes measured the raw output of resistivity to electrical current in Ω-m. Calibration curves were generated by mixing known molar masses of readily available food-grade NaCl (i.e., table salt) with ultrapure water (Milli-Q, 18.2 MΩ-cm) for concentrations that encompassed the experimental concentrations. Measured resistivity was inversed and adjusted such that calibrations curves were best-fit between electrical conductance (mS/m) and chloride concentration (mg/L). Linear relationships were investigated but found to be inaccurate for concentrations below 200 mg/L, and thus exponential functions [chloride concentration = a*(electrical conductance)^b] were used. A separate calibration curve was created and used for each column and for the supply tank. Calibrations were checked prior to each salt-laden application. The fitting parameters for the calibration curves varied as follows: $349.9 < a < 525.8$; $1.092 < b < 1.297$; $0.965 < r^2 < 0.996$.

3.2 FIELD CORE COLLECTION

Field cores were collected using a Geo Probe 7800 probe with augers in two locations along Highway 52 in Mendota Heights, MN; one targeting sandy loam soil and another targeting silt loam. The first

location (SB-1) is located along the southbound lanes of highway 52, approximately where 67th Street E would intersect the highway if it continued beyond the cul-de-sac (see Figure 1). The soil in this location is categorized as soil type: 896 (Kingsley-Mahtomedi Complex) which is primarily sandy loam (USDA NRCS Web soil survey https://websoilsurvey.sc.egov.usda.gov/App/WebSoilSurvey.aspx). The second location (SB-2) for field cores is located just south of 75th Street E along the southbound lanes of Highway 52 in Mendota Heights, MN. The soil in this location is categorized as soil type: 344 (silt loam). (USDA NRCS Web soil survey https://websoilsurvey.sc.egov.usda.gov/App/WebSoilSurvey.aspx).

Figure 1. Field core site SB-1 (left), Highway 52 & 67th Street Sandy Loam soil type: 896 (Kingsley-Mahtomedi Complex); and site SB-2 (right), Highway 52 & 75th Street at mile marker #123; Silt Loam soil type: 344 (silt loam). Top photos illustrate geographic location (Courtesy https://websoilsurvey.sc.egov.usda.gov/App/WebSoilSurvey.aspx) while bottom photos illustrate street view (courtesy https://www.google.com/maps).

At each of these two sites, four cores were collected from the edge of the highway to the backslope of the ditch. The first was collected near the edge of the pavement, the second approximately midslope between pavement and bottom of the ditch, the third in the bottom of the ditch, and the fourth approximately midslope on the side of the ditch furthest from the roadway. The cores that were collected were approximately 2.5 cm in diameter and collected in two segments; one from a depth of 0 – 1.5 m and another from 1.5 m to 3 m. Due to the collection process (core penetration into the soil), the soil within the cores became compressed by various amounts. Thus, the final cores were 2.5 cm in diameter and varied in length from 1.27 m to 2.44 m. Each segment was adjusted linearly back to 1.5 m in length by assuming that the compression ratio was constant with depth.

After extraction, each field core was segmented into four to seven soil horizons by visual indicators such as color, grain size, organic content, etc. Each segment varied in length between 5 cm and 1.32 m. The

soil from each segment was homogenized and submitted to the Research Analytical Laboratories (http://ral.cfans.umn.edu/) for analysis of chloride content (mg/kg), organic matter (percent loss on ignition), cation exchange capacity (meg/100g), saturation extractable electrical conductivity (mmhos/cm), sodium adsorption ratio (SAR), exchangeable sodium (%), total organic carbon (% C), soil texture (% sand, % silt, % clay), and pH when soaked in water.

3.3 MODELING

To further characterize and understand the transport of chloride in the soil columns, one-dimensional computer simulations were performed using the Hydrus 1-D modeling software (Simunek, van Genuchten, & Sejna, 2016). The Hydrus package enables the simulation of water and solute transport through soil using either linear or non-linear transport equations. For this study, models were assembled for the experimental soil columns, and chloride loading and flushing events were simulated. The hydraulic and solute transport parameters in each Hydrus model was adjusted to match the observed water flow rates and chloride concentrations, e.g. the chloride breakthrough curves

Each model assumed a 25 cm long, saturated soil column with 10 feet of head loading the column top and atmospheric pressure at the lower end of the column. Water transport was simulated using the van Genuchten-Mualem model (van Genuchten, 1980) in Hydrus. Since the soil columns were saturated, only the soil porosity and saturated hydraulic conductivity needed to be calibrated. The saturated hydraulic conductivity was set based on the slope of the observed water flow rate vs. time in the soil columns. The soil prosody was one of four parameters adjusted to match the observed breakthrough curves.

Chloride transport through the soil columns was simulated in Hydrus using the dual-porosity, mobile-immobile model. This model assumes that a fixed fraction of the soil pores do not actively contribute to water transport, but are connected to the active pores and can exchange solute via diffusion (Figure 2). The immobile pore fraction and the rate coefficient for solute exchange between the active and inactive pores were two of the four calibration parameters for the Hydrus models.

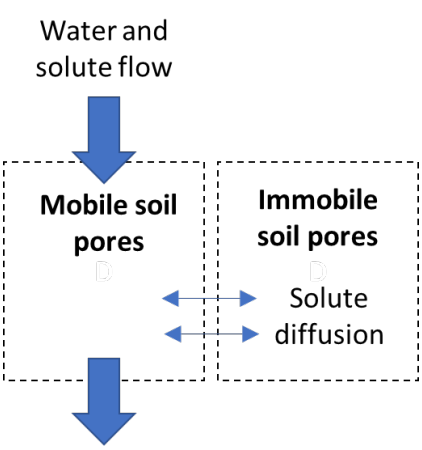

Figure 2: Schematic diagram for the mobile-immobile solute transport model using in this study.

For each simulation, the initial chloride concentration in the column was set based on the initial measured chloride concentration at the column outlet. The chloride input concentration to the column

was set based on the final observed concentration at the column outlet, assuming that input and output concentration reach equilibrium given sufficient time. For shorter runs where the observed outlet concentration did not reach an equilibrium, the input concentration was an additional calibration parameter.

Hydrus simulations were run for a subset of experimental runs, including chloride loading and flushing runs for all three soil types (sandy loam, silt loam, and sandy loam with 10% organic). After setting the saturate hydraulic conductivity, initial chloride concentration, and input chloride concentration, very good fits of the chloride breakthrough curves were obtained by adjusting four calibration parameters: the total soil porosity, the immobile pore fraction, the chloride diffusivity parameter, and the rate constant for diffusion to the immobile pores. The best model fit to the observed breakthrough curve was determined by minimizing the root-mean-square error (RMSE) parameter.

CHAPTER 4: RESULTS AND DISCUSSION

4.1 COLUMN EXPERIMENTS

4.1.1 Silt Loam

During these experiments there were five phases in which each phase consisted of a salt-laden loading portion and a salt-free rinse portion. Phase 1 for the silt loam soil is shown in Figure 3. Soon after the initial addition of salt to the columns, the first replicate (column 1) of silt loam (Rep1, Col1 in Figure 3) demonstrated a substantial reduction in flow rate. This is likely due to the interaction between the sodium from the NaCl salt in the influent and the clay content in the soil (~15% clay), which dispersed clay particles that clogged the column. A reduction in flow rate was observed in all columns, but not to the extent as was observed in column 1. As a result, column 1 would not reach steady state with the influent in a reasonable amount of time. Thus, column 1 is excluded from further discussion.

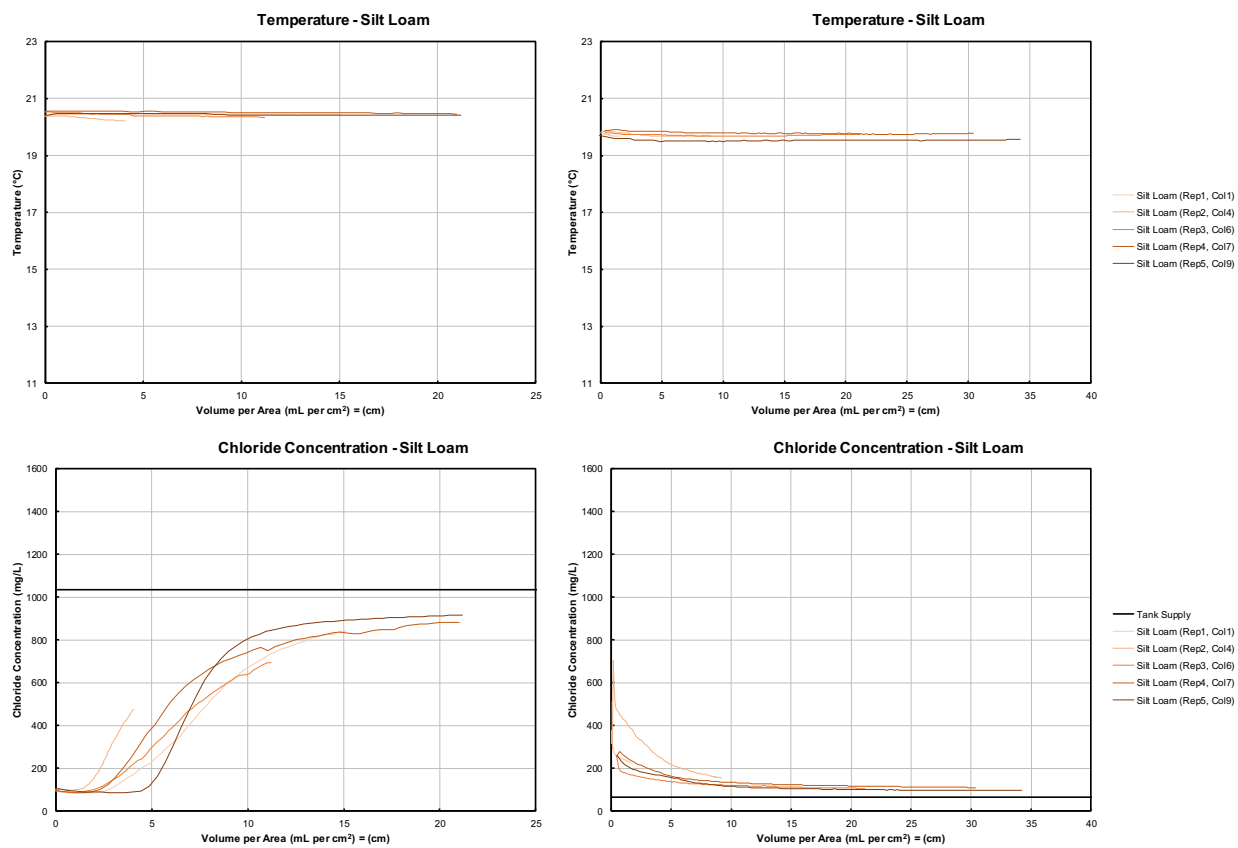

Figure 3. Temperature (top) and Chloride (bottom) data for Phase 1 on silt loam columns. Salt-laden loading (left) and salt-free rinse (right). On average, one pore volume for the silt loam columns is ~ 7 mL per cm^2.

As shown in Figure 3, the effluent concentration from the silt loam columns during salt loading was always less than the influent concentration. In the case of replicates 4 and 5, the effluent concentration was ~80% of the influent concentration after 20 cm (~3 pore volumes). As described in the methods section above, each cm is approximately equivalent to one year of percolation from precipitation in Minnesota. If salt were completely conservative and all the soil pores were transmissive, then the

effluent concentration should become equal to the influent concentration within a few pore volumes. For replicates 4 and 5 of the silt loam columns, the effluent concentration appears to approach steady state because there is minimal change as water continues to flow through the soil. The effluent concentration reaches steady state at a concentration less than the influent, which suggests that salt is being stored within the soil column. During the salt-free rinse portion, the effluent concentration was always greater than the influent concentration, for some columns after flushing with greater than 30 cm (~ 4 pore volumes). The effluent concentration from replicates 4 and 5 was approximately 50% greater than the influent concentration. This suggests that salt stored within the columns during salt loading was released during the salt-free rinse.

Phase 2 was initially mixed at a salt concentration of approximately 644 mg/L, and then a second salt-laden loading portion was applied with a supply concentration of approximately 984 mg/L, followed by a salt-free rinse portion. The results for silt loam columns are shown in Figure 4.

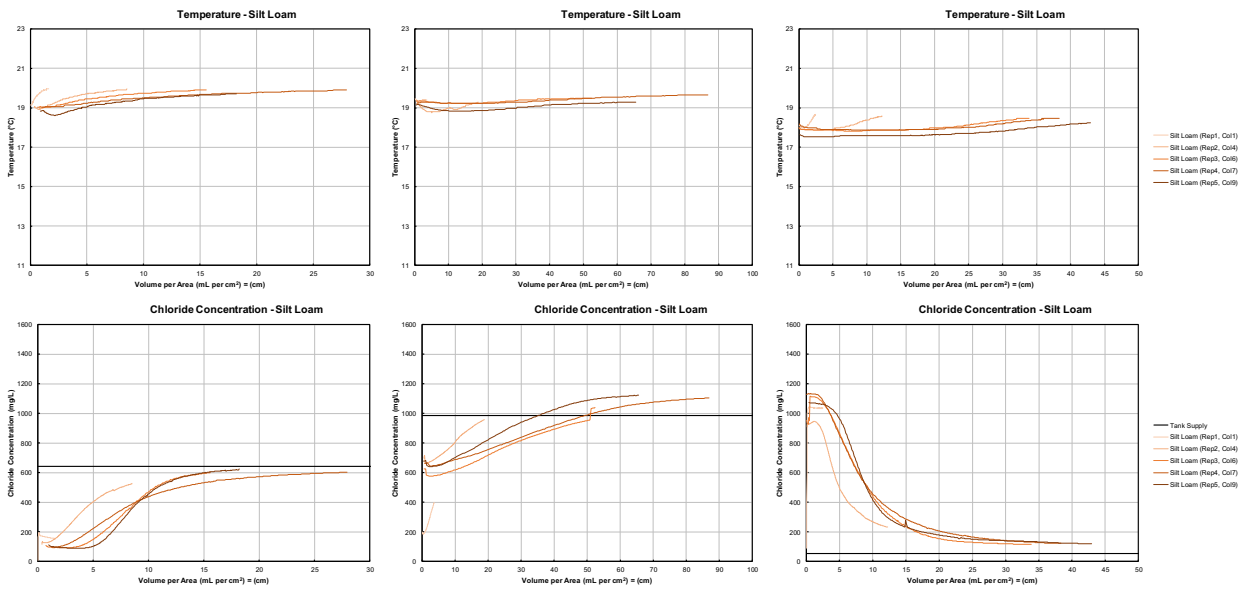

Figure 4. Temperature (top) and Chloride (bottom) data for Phase 2 on silt loam columns. Salt-laden loading (left and center) and salt-free rinse (right). On average, one pore volume for the silt loam columns is ~ 7 mL per cm^2.

During the first salt loading of Phase 2 (i.e., 644 mg/L), the silt loam columns reached approximately 95% of the influent concentration within 15 – 25 cm (2.5 – 4 pore volumes, Figure 4 bottom left). During the second salt loading of Phase 2 (i.e., 984 mg/L, Figure 4 bottom center), the effluent concentration began to exceed the influent concentration after 35 – 50 cm (5 – 7 pore volumes) and eventually exceeded the effluent by ~14% after 65 – 85 cm (9 – 12 pore volumes). This suggests that salt is stored within the soil and released during the second salt loading of Phase 2; but this is inconsistent with the first salt loading of Phase 2 (Figure 4 bottom left) because the effluent appears to be approaching steady state at the influent concentration, which is substantially less than the influent concentration of the second salt loading of Phase 2. In addition, the second salt loading run resulted in effluent concentrations that are higher than the influent concentrations. This is only possible if chloride was adsorbed to the silt loam, only to be released later during the second run. If salt were stored within the silt loam columns, it would be expected to be released during the first salt loading of Phase 2, not the second. The effluent salt concentration was approximately twice the influent concentration during the salt-free rinse (Figure 4

bottom right) after 30 – 40 cm (4 – 6 pore volumes). This also suggests that salt was stored within the soil column and was released during the salt-free rinse as seen in Phase 1.

The salt loading in Phase 3 also suggests salt is stored within the columns because the effluent concentration appears to reach steady state at ~80% of the influent concentration after 30 cm (~4 pore volumes, Figure 5 bottom left). As was observed in Phases 1 and 2, this salt appears to be released during the salt-free rinse (Figure 5 bottom right) because the effluent concentration approaches steady state at a concentration approximately twice the concentration of the influent after 35 – 40 cm (5 – 6 pore volumes).

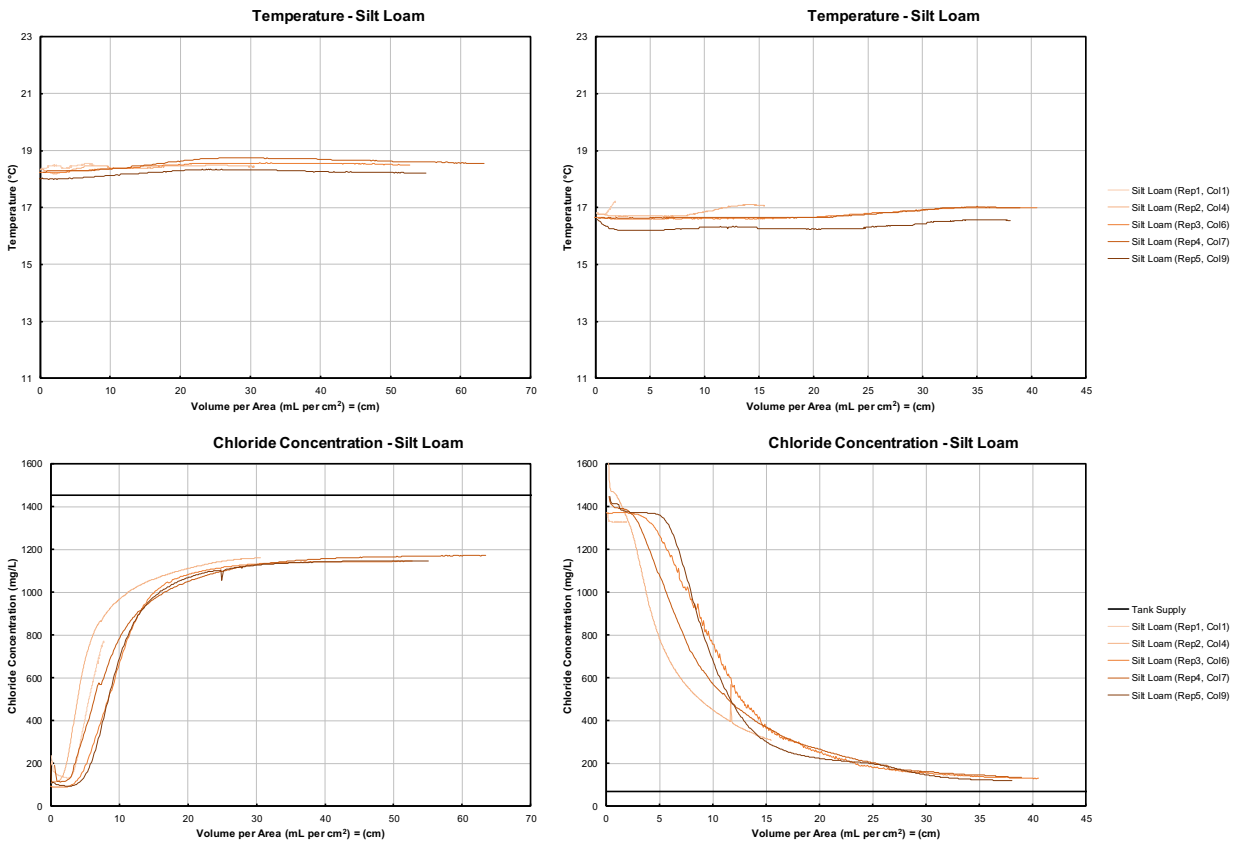

Figure 5. Temperature (top) and Chloride (bottom) data for Phase 3 on silt loam columns. Salt-laden loading (left) and salt-free rinse (right). On average, one pore volume for the silt loam columns is ~ 7 mL per cm^2.

Phases 4 (Figure 6) and 5 (Figure 7) of the silt loam columns both demonstrate salt release during both salt loading (bottom left) and salt-free rinse (bottom right) because the effluent concentration is greater than the influent concentration. It's possible that the high influent concentration during the salt loading in Phase 3 (~1450 mg/L) contributed substantial salt to the less active pores within the silt loam, which was later released during the salt loading (influent concentration ~1015 – 1020 mg/L) and salt-free rinse (influent concentration ~60 – 65 mg/L) portions of Phases 4 and 5.

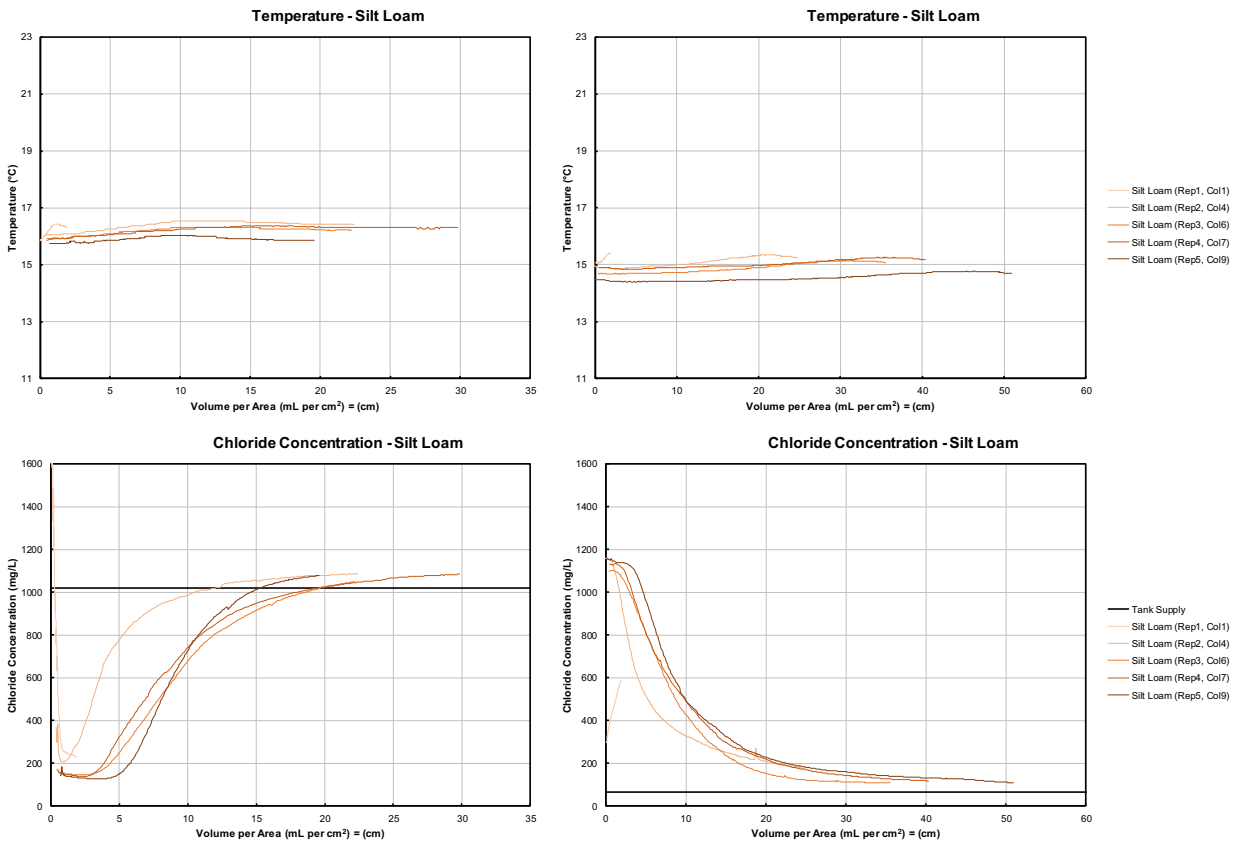

Figure 6. Temperature (top) and Chloride (bottom) data for Phase 4 on silt loam columns. Salt-laden loading (left) and salt-free rinse (right). On average, one pore volume for the silt loam columns is ~ 7 mL per cm².

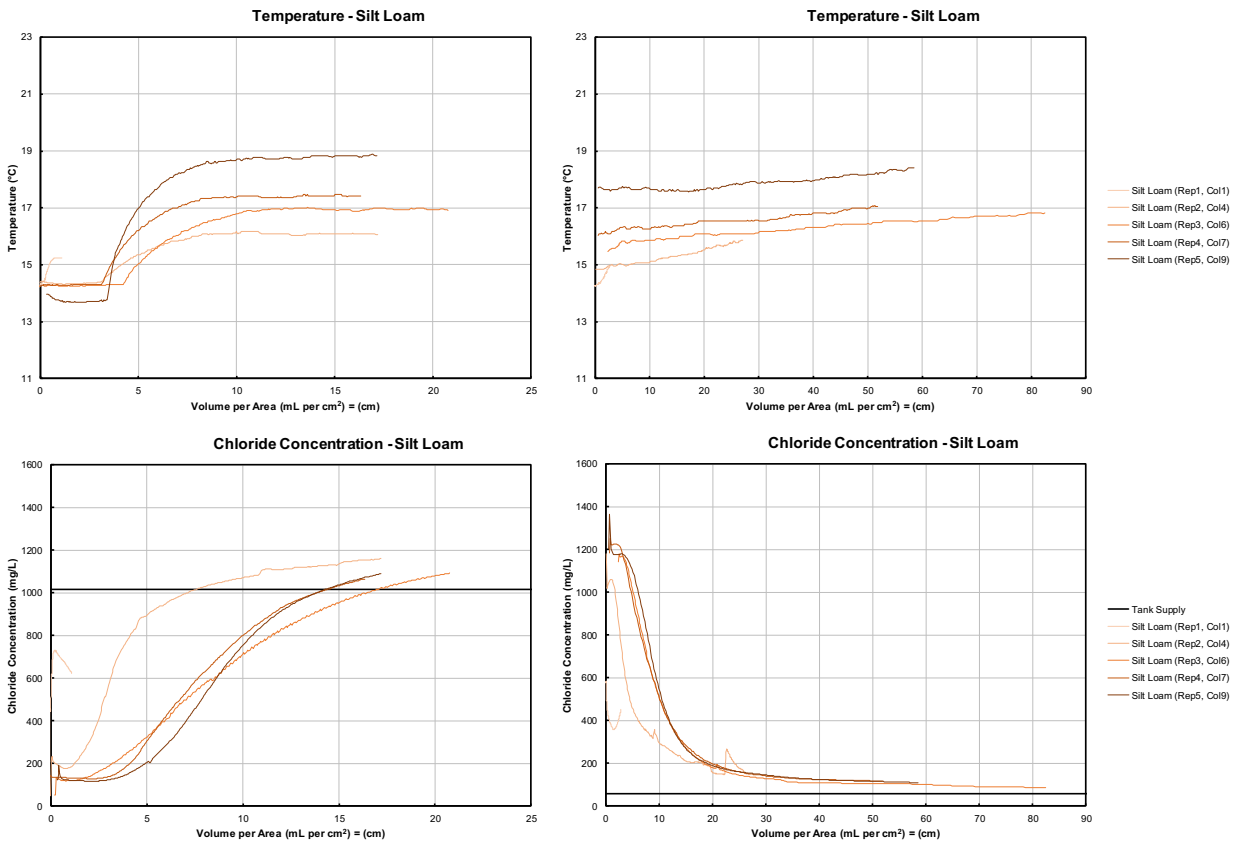

Figure 7. Temperature (top) and Chloride (bottom) data for Phase 5 on silt loam columns. Salt-laden loading (left) and salt-free rinse (right). On average, one pore volume for the silt loam columns is ~ 7 mL per cm².

4.1.2 Sandy Loam

Phase 1 for sandy loam columns is shown in Figure 8. Similar to the observations in the silt loam columns, the Phase 1 for the sandy loam columns suggests that salt is stored within the column during salt loading (Figure 8 bottom left) because the effluent concentration approaches steady state at about 85 – 90% of the influent concentration after about 30 cm (4 pore volumes). In the salt-free rinse (Figure 8 bottom right) the effluent concentration approached steady state after 10 – 20 cm (2 – 3 pore volumes) at about a concentration about 50% greater than the influent, suggesting salt stored in the columns is released during the rinse.

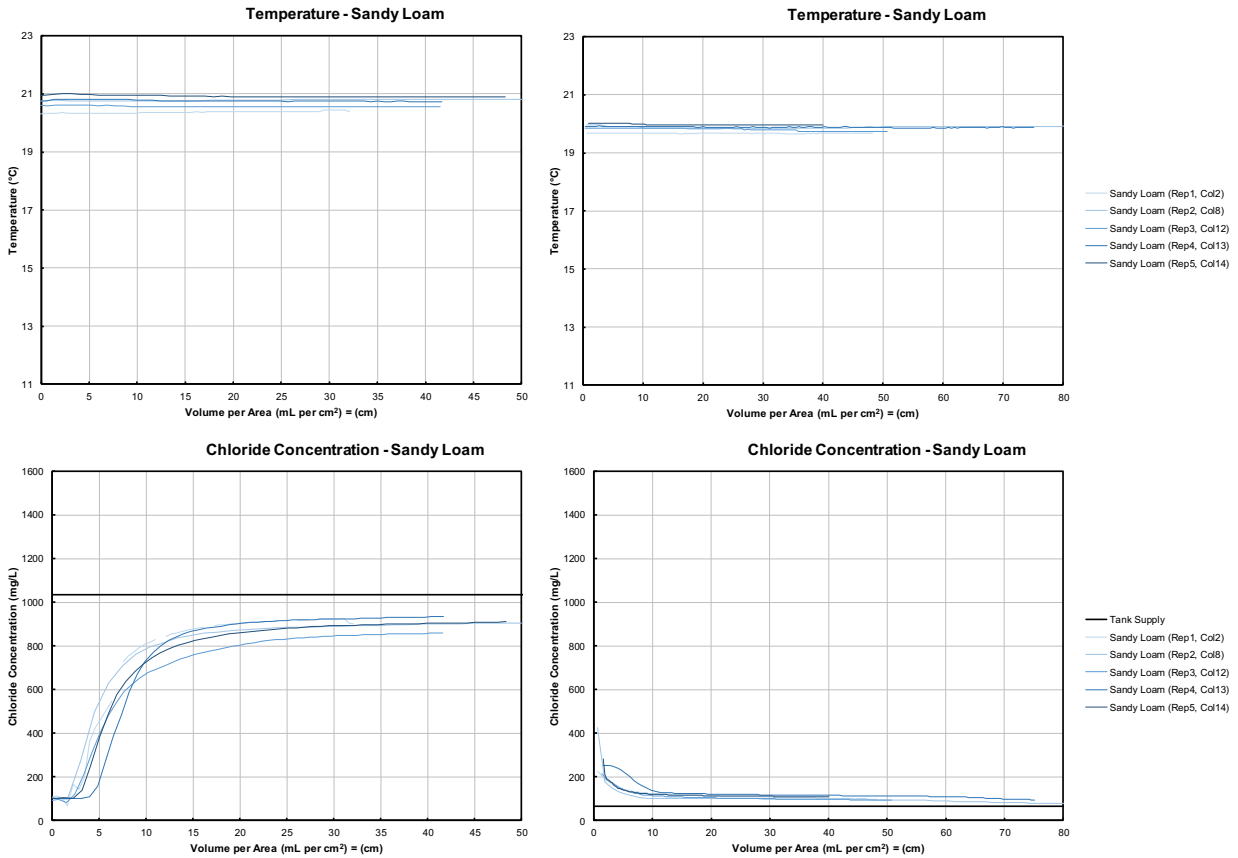

Figure 8. Temperature (top) and Chloride (bottom) data for Phase 1 on sandy loam columns. Salt-laden loading (left) and salt-free rinse (right). On average, one pore volume for the sandy loam columns is ~ 7.2 mL per cm².

In Phase 2, as was observed for the silt loam columns, the sandy loam columns reached approximately 95% of the influent concentration after 25 cm (~3.5 pore volumes, Figure 9 bottom left) for three out of the five replicates in the first salt loading of the phase. Replicates 2 and 3 approached steady state at a substantially lower fraction of the influent; 65% and 75%, respectively. It is unclear why these replicates behaved differently than the others. During the second salt loading of Phase 2 (Figure 9 bottom center), the effluent concentration began to exceed the influent concentration after 40 – 60 cm (5.5 – 8 pore volumes) and eventually exceeded the effluent by ~18% after 90 – 150 cm (12.5 – 21 pore volumes). This suggests that salt is stored within the soil and released during the second salt loading; but this is inconsistent with the first salt loading of Phase 2 (Figure 9 bottom left) because the effluent appears to be in steady state at the influent concentration, which is substantially less than the influent concentration of the second salt loading. If salt were stored within the sandy loam columns, it would be expected to be released during the first salt loading, not the second. The effluent salt concentration was approximately twice the influent concentration during the salt-free rinse (Figure 9 bottom right) after 10 – 20 cm (1.5 – 3 pore volumes). This also suggests that salt was stored within the soil column and was released during the salt-free rinse as seen in Phase 1.

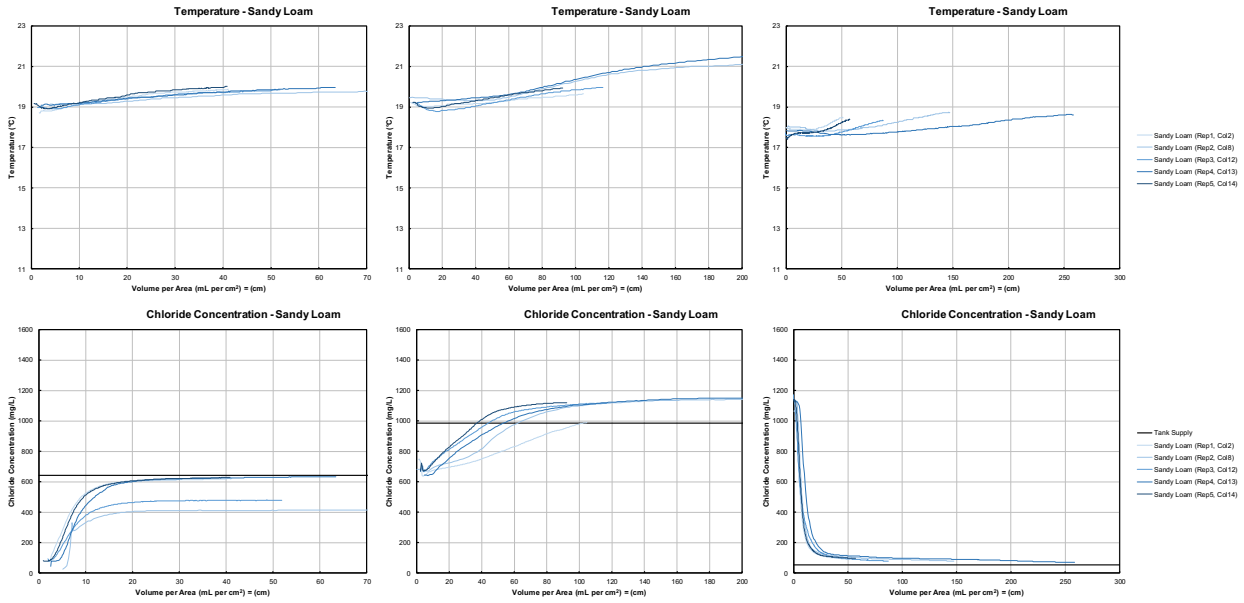

Figure 9. Temperature (top) and Chloride (bottom) data for Phase 2 on sandy loam columns. Salt-laden loading (left and center) and salt-free rinse (right). On average, one pore volume for the sandy loam columns is ~ 7.2 mL per cm^2.

The salt loading in Phase 3 also suggests salt is stored within the columns because the effluent concentration appears to reach steady state at ~85 – 90% of the influent concentration after 90 – 150 cm (12.5 – 21 pore volumes, Figure 10 bottom left). As was observed in Phases 1 and 2, this salt appears to be released during the salt-free rinse (Figure 10 bottom right) because the effluent concentration reaches steady state at a concentration approximately twice the concentration of the influent after 60 cm (8 pore volumes).

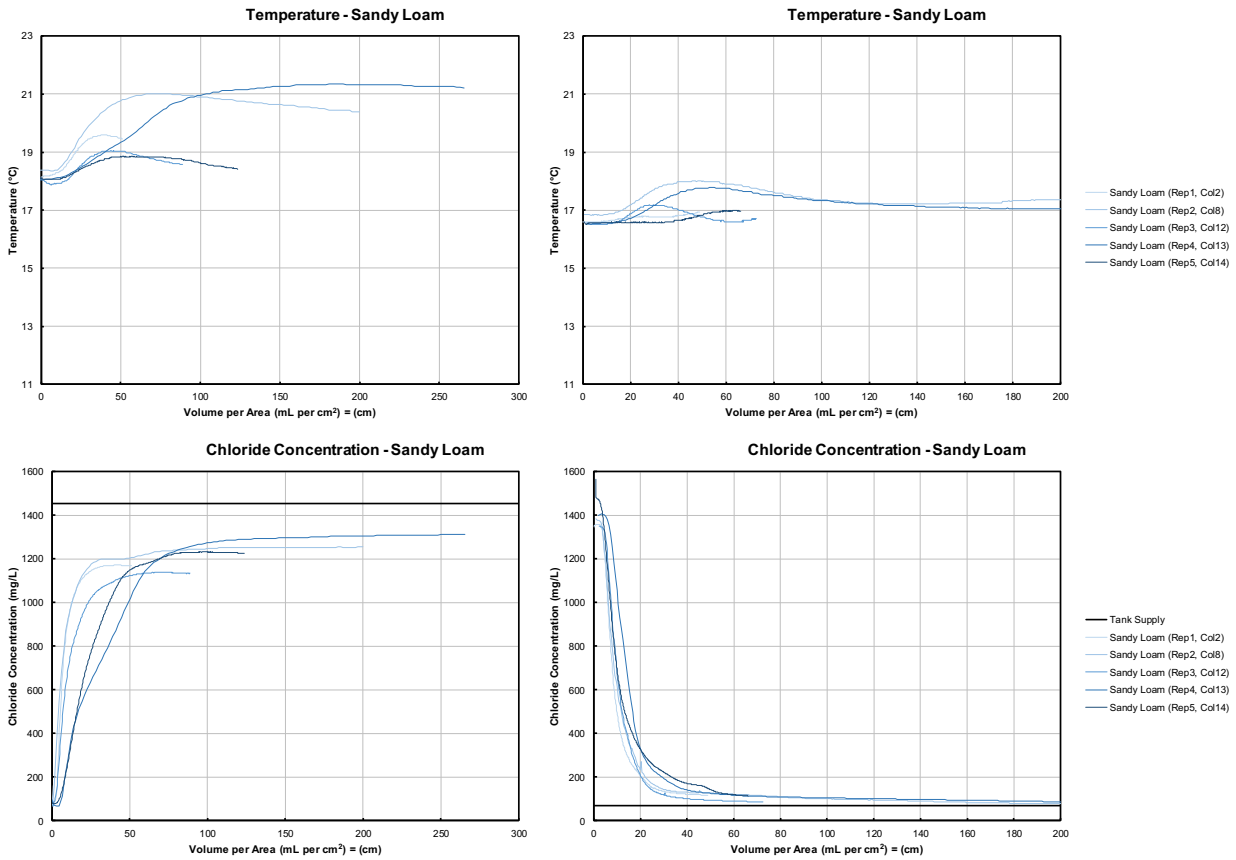

Figure 10. Temperature (top) and Chloride (bottom) data for Phase 3 on sandy loam columns. Salt-laden loading (left) and salt-free rinse (right). On average, one pore volume for the sandy loam columns is ~ 7.2 mL per cm².

Phases 4 (Figure 11) and 5 (Figure 12) of the sandy loam columns both demonstrate salt release during both salt loading (bottom left) and salt-free rinse (bottom right) because the effluent concentration is greater than the influent concentration. It's possible that the high influent concentration during the salt loading in Phase 3 (~1450 mg/L) contributed substantial salt to the less active pores within the sandy loam, which was later released during the salt loading (influent concentration ~1015 – 1020 mg/L) and salt-free rinse (influent concentration ~60 – 65 mg/L) portions of Phases 4 and 5. This behavior was also observed in the silt loam soil (Figure 6 & Figure 7) above.

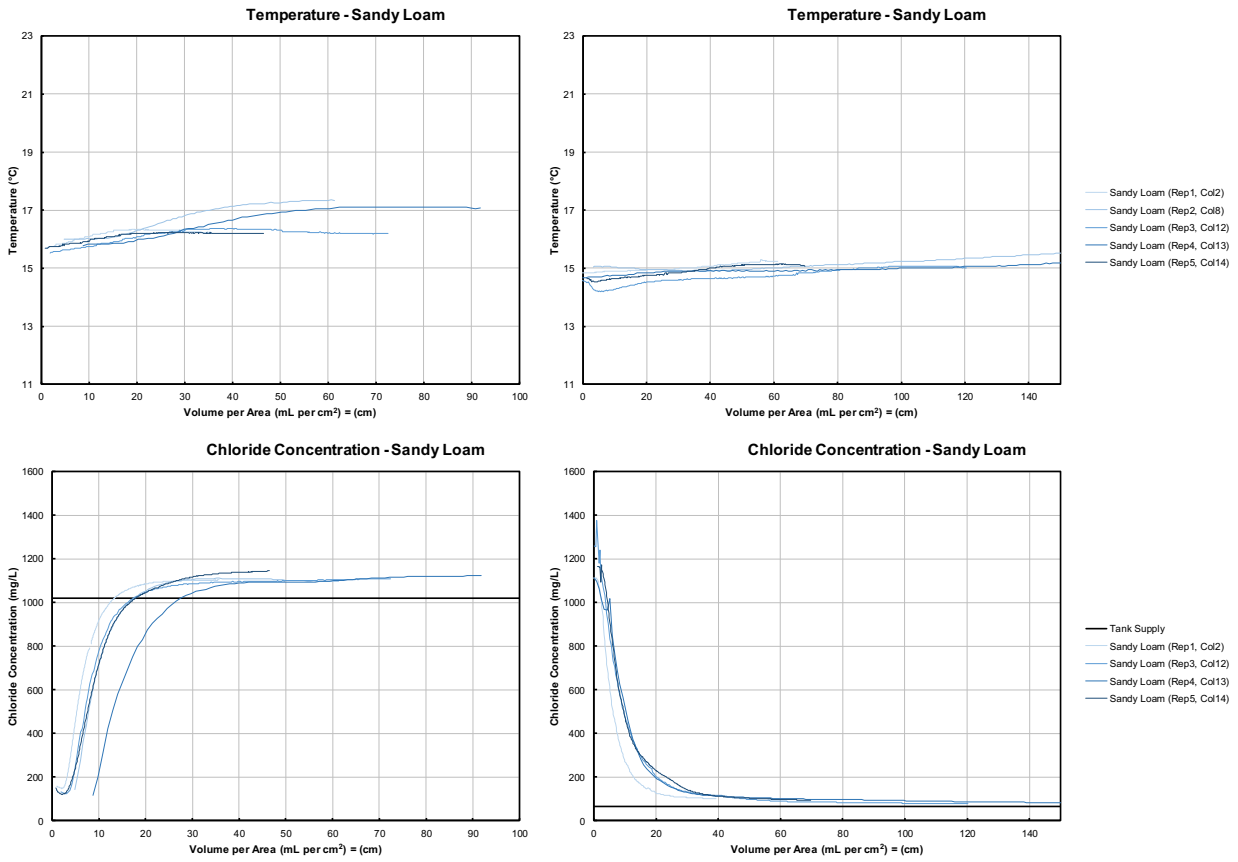

Figure 11. Temperature (top) and Chloride (bottom) data for Phase 4 on sandy loam columns. Salt-laden loading (left) and salt-free rinse (right). On average, one pore volume for the sandy loam columns is ~ 7.2 mL per cm².

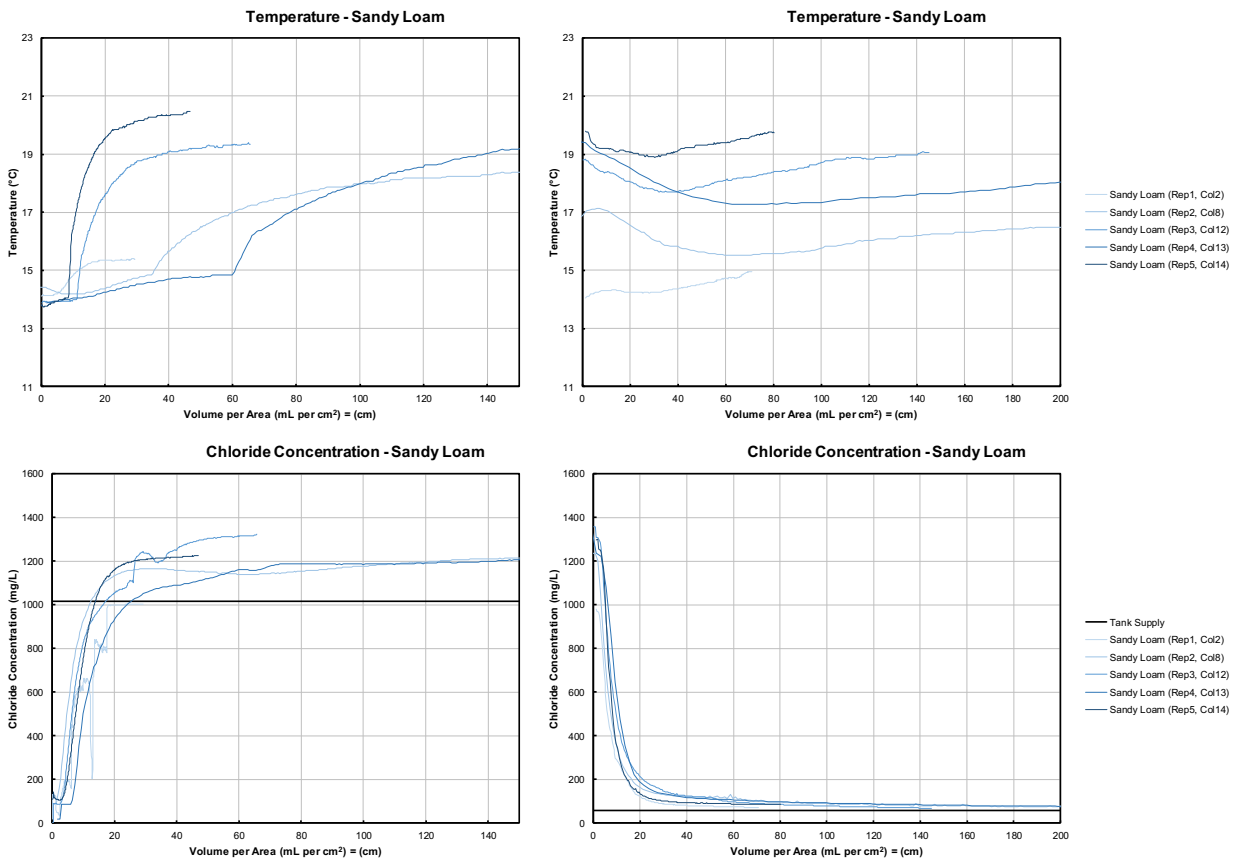

Figure 12. Temperature (top) and Chloride (bottom) data for Phase 5 on sandy loam columns. Salt-laden loading (left) and salt-free rinse (right). On average, one pore volume for the sandy loam columns is ~ 7.2 mL per cm².

4.1.3 Sandy Loam with 10% Organic

Phase 1 for sandy loam with 10% organic columns is shown in Figure 13. Similar to the observations in the silt loam and sandy loam columns, the Phase 1 for the sandy loam with 10% organic columns suggests that salt is stored within the column during salt loading (Figure 13 bottom left) because the effluent concentration approaches steady state at about 80 – 90% of the influent concentration after about 30 cm (4 pore volumes). In the salt-free rinse (Figure 13 bottom right) the effluent concentration decreased to below 100 mg/L (influent concentration ~65 mg/L) within 20 mL (2.5 pore volumes) but then decreased to below 80 mg/L after 80 cm (10.5 pore volumes). By 150 cm (20 pore volumes) the effluent concentration approached steady state at 50 – 75 mg/L, with two of the column replicates having effluent concentrations less than the influent and three replicates having effluent concentrations greater than the influent. This suggests that salt is stored during salt loading and released during salt-free rinse but that the columns are effectively at steady state with the influent after a long flow-through period (~20 pore volumes).

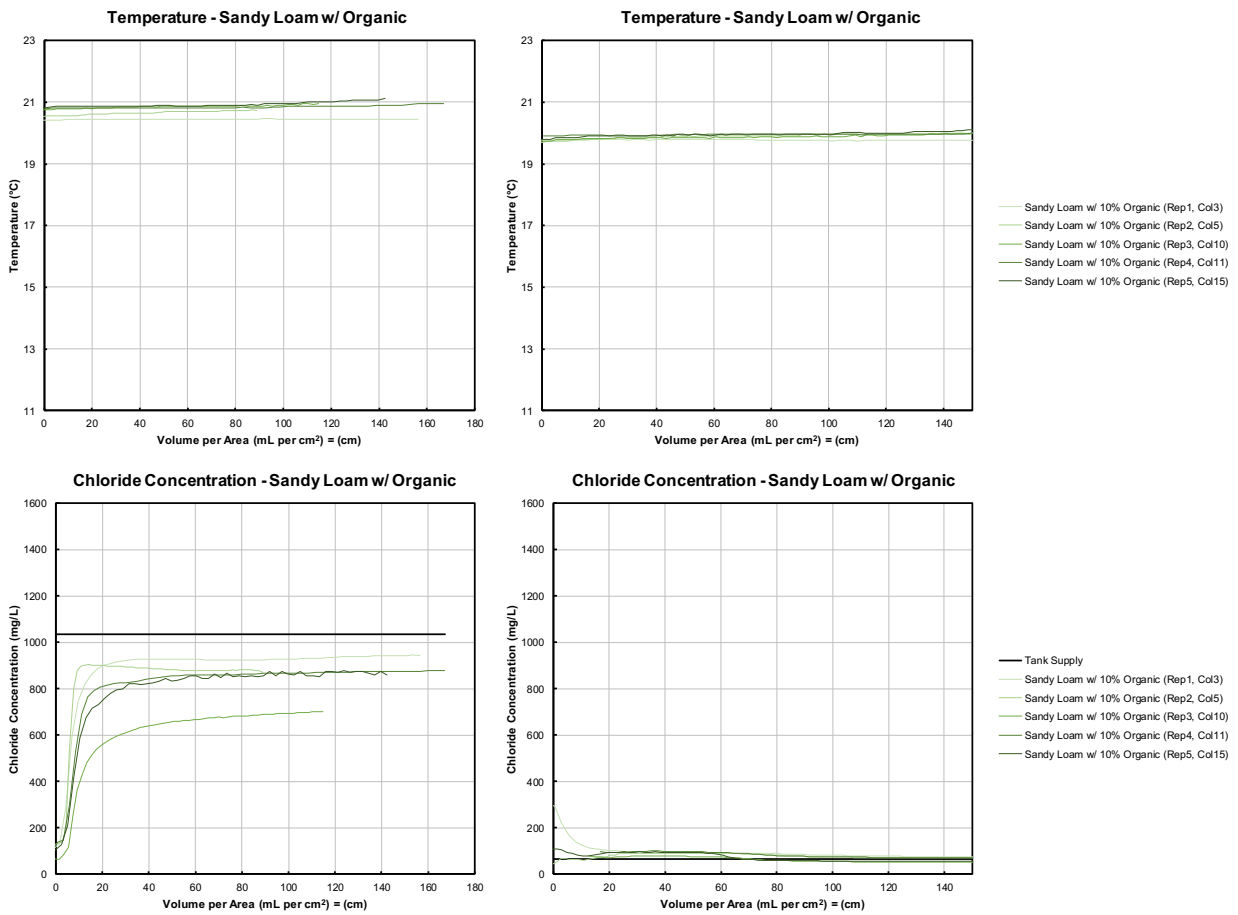

Figure 13. Temperature (top) and Chloride (bottom) data for Phase 1 on sandy loam with 10% organic columns. Salt-laden loading (left) and salt-free rinse (right). On average, one pore volume for the sandy loam with 10% organic columns is ~ 7.6 mL per cm^2.

As was observed for the silt loam and sandy loam columns, the effluent from the sandy loam with 10% organic columns reached approximately 85 – 95% of the influent concentration after 30 cm (~4 pore volumes, Figure 14 bottom left) during the first salt loading of Phase 2. Replicates 3 and 5, though, required substantially more depth to approach steady state; 50 cm (6.5 pore volumes) and 250 cm (33 pore volumes), respectively. It is unclear why these replicates behaved differently than the others. During the second salt loading of Phase 2 (Figure 14 bottom center), the effluent concentration began to exceed the influent concentration after 60 – 150 cm (8 – 20 pore volumes) and eventually exceeded the effluent by 10 – 18% after 150 cm (20 pore volumes). This suggests that salt is stored within the soil and released during the second salt loading of Phase 2; but this is inconsistent with the first salt loading of Phase 2 (Figure 14 bottom left) because the effluent appears to at steady state below the influent concentration, which is substantially less than the influent concentration of the second salt loading. If salt were stored within the sandy loam columns, it would be expected to be released during the first salt loading of the phase, not the second. The effluent salt concentration becomes approximately equivalent to the influent concentration after 140 – 200 cm (20 – 26 pore volumes, Figure 14 bottom right). As observed in Phase 1 for the sandy loam with 10% organic, this suggests that salt is stored during salt loading and released during salt-free rinse but that the columns are effectively at steady state with the influent after a long flow-through period (~20 pore volumes).

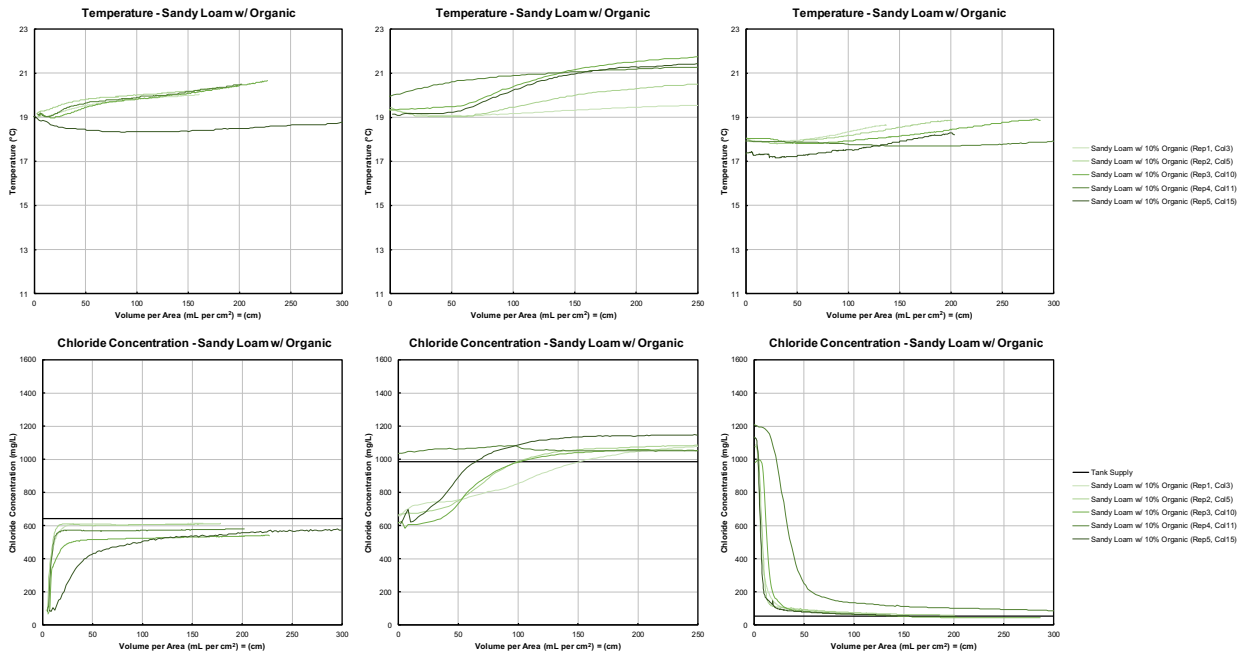

Figure 14. Temperature (top) and Chloride (bottom) data for Phase 2 on sandy loam with 10% organic columns. Salt-laden loading (left and center) and salt-free rinse (right). On average, one pore volume for the sandy loam with 10% organic columns is ~ 7.6 mL per cm^2.

The salt loading in Phase 3 also suggests salt is stored within the columns because the effluent concentration appears to approach steady state at ~80 – 90% of the influent concentration after 40 cm (5 pore volumes) for replicates 1 and 2, after 80 cm (10.5 pore volumes) for replicate 4, and after 150 cm (20 pore volumes) for replicates 3 and 5 (Figure 15 bottom left). During the salt-free rinse (Figure 15 bottom right) the effluent salt concentration is greater than the influent concentration suggesting that previously stored salt is released until about 100 cm (13 pore volumes). After this the effluent during the rinse becomes approximately equivalent to the influent concentration suggesting steady state with the influent at this concentration as was observed in Phases 1 and 2 for the sandy loam with 10% organic.

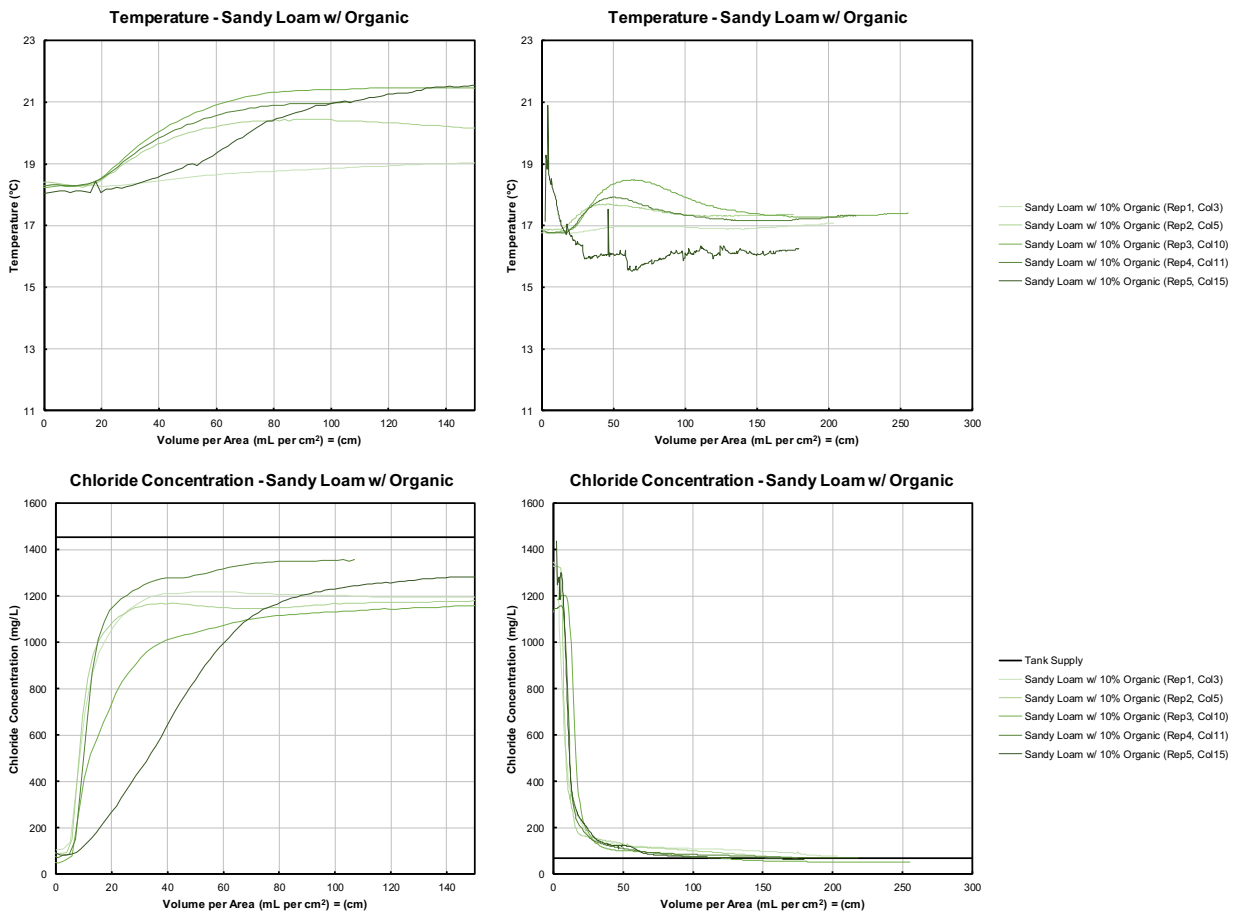

Figure 15. Temperature (top) and Chloride (bottom) data for Phase 3 on sandy loam with 10% organic columns. Salt-laden loading (left) and salt-free rinse (right). On average, one pore volume for the sandy loam with 10% organic columns is ~ 7.6 mL per cm^2.

Phases 4 (Figure 16) and 5 (Figure 17) of the sandy loam with 10% organic columns both demonstrate salt release during both salt loading (bottom left) and salt-free rinse (bottom right) because the effluent concentration is greater than the influent concentration. It's possible that the high influent concentration during the salt loading in Phase 3 (~1450 mg/L) contributed substantial salt to the less active pores within the sandy loam with 10% organic, which was later released during the salt loading (influent concentration ~1015 – 1020 mg/L) and salt-free rinse (influent concentration ~60 – 65 mg/L) portions of Phases 4 and 5. This behavior was also observed in the silt loam soil (Figure 6 & Figure 7) and sandy loam (Figure 11& Figure 12) above.

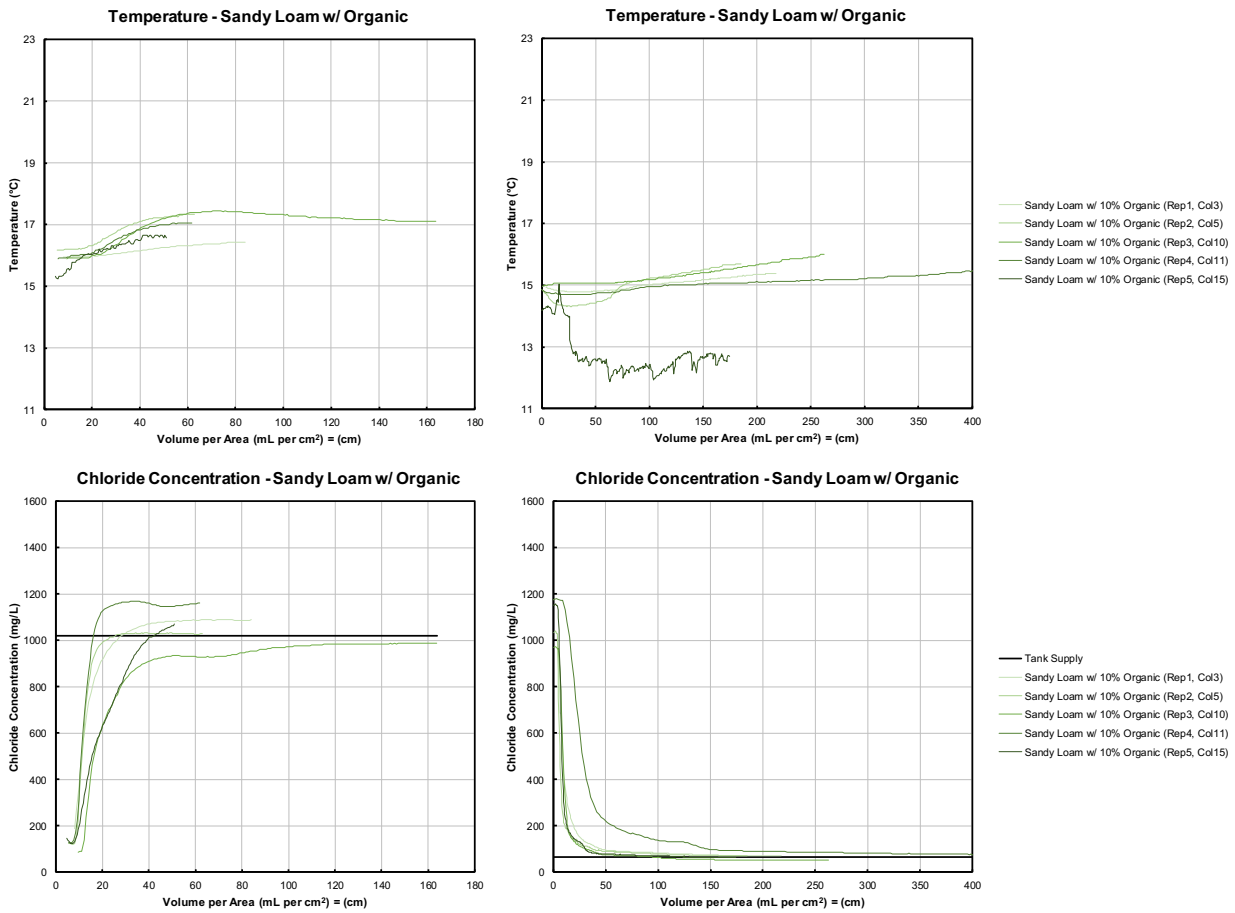

Figure 16. Temperature (top) and Chloride (bottom) data for Phase 4 on sandy loam with 10% organic columns. Salt-laden loading (left) and salt-free rinse (right). On average, one pore volume for the sandy loam with 10% organic columns is ~ 7.6 mL per cm^2.

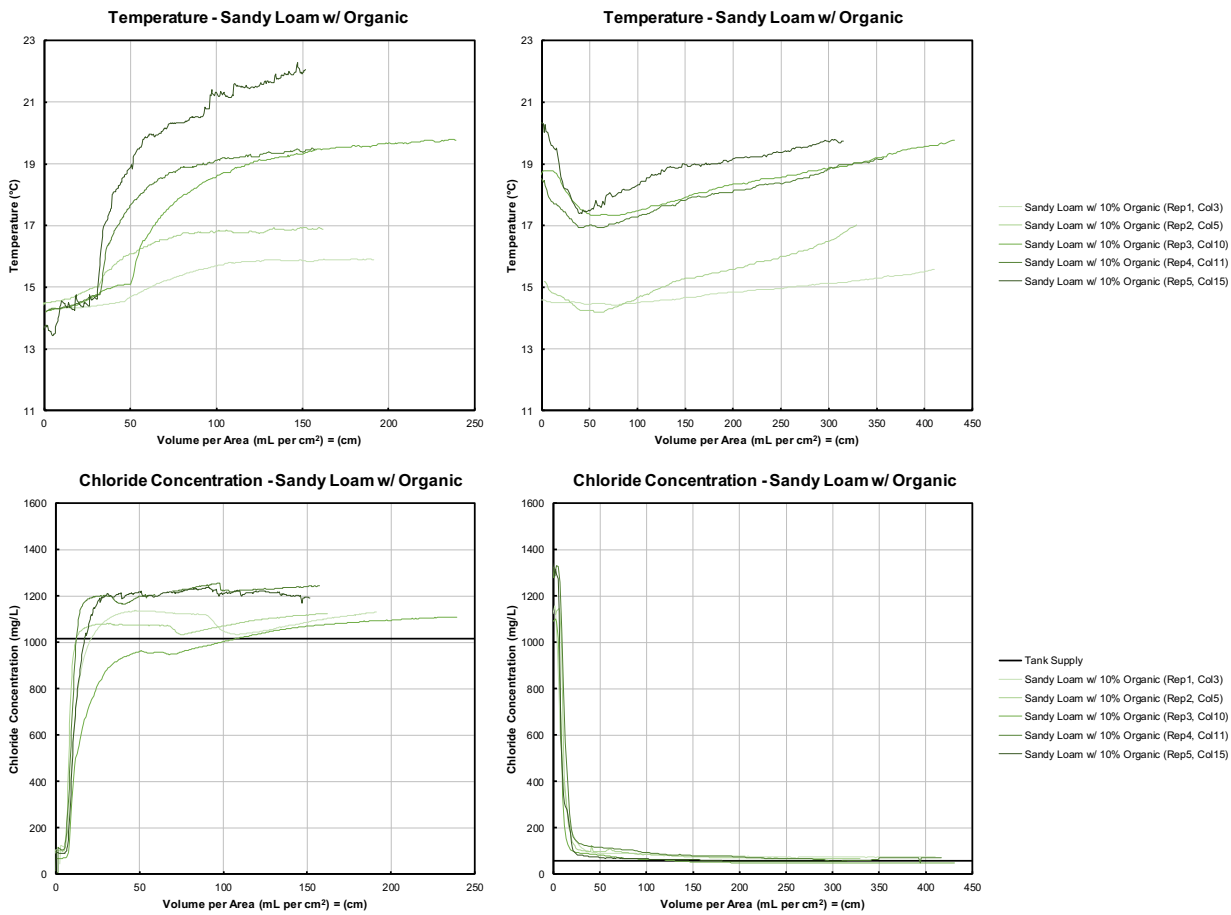

Figure 17. Temperature (top) and Chloride (bottom) data for Phase 5 on sandy loam with 10% organic columns. Salt-laden loading (left) and salt-free rinse (right). On average, one pore volume for the sandy loam with 10% organic columns is ~ 7.6 mL per cm^2.

4.2 FIELD CORES

As described above, field cores were collected, segmented, and analyzed for various soil parameters. The following plots illustrate the soil properties as a function of site (SB-1: sandy loam; or SB-2: silt loam), location (A = near the edge of the pavement, B = midslope between pavement and bottom of the ditch, C = in the bottom of the ditch, D = midslope on the side of the ditch furthest from the roadway), and soil depth.

The soil texture classification in the field cores is listed and illustrated in Table 1. Although soil survey data suggested sandy loam at site SB-1 and silt loam at site SB-2, both sites were found to be primarily sandy clay loam. A section of loam is present at depths greater than 180 cm in location B for site SB-1 and location D for site SB-2. There is also a section of sandy loam in site SB-1 at 150 – 180 cm deep in location C (ditch bottom) and from 20 – 70 cm deep in location D (backslope). The presence of sandy clay loam in both field core sites means that the two sites cannot be necessarily differentiated by soil type as was intended when the sites were selected. The soil types present also do not correspond with the soil types used in the column experiments.

Table 1: Soil texture classification for Site SB-1: Sandy Loam (left) and SB-2: Silt Loam (right). A = near the edge of the pavement, B = midslope between pavement and bottom of the ditch, C = in the bottom of the ditch, D = midslope on the side of the ditch furthest from the roadway.

Depth	Site SB-1: Highway 52 & 67th Street; Sandy Loam Soil type: 896 (Kingsley-Mahtomedi Complex)				Site SB-2: Highway 52 & 75th Street; Silt Loam Soil type: 344 (silt loam)			
(cm)	A	B	C	D	A	B	C	D
0 - 10	Sandy Clay Loam	Sandy Clay Loam	Sandy Clay Loam	Sandy Clay Loam	Sandy Clay Loam	Sandy Clay Loam	Sandy Clay Loam	Sandy Clay Loam
11 - 20						Sandy Clay Loam		
21 - 30	Sandy Clay Loam	Sandy Clay Loam		Sandy Loam	Sandy Clay Loam			Sandy Clay Loam
31 - 40			Sandy Clay Loam					
41 - 50				Sandy Loam		Sandy Clay Loam		
51 - 60		Sandy Clay Loam			Sandy Clay Loam			
61 - 70			Sandy Clay Loam	Sandy Loam				Sandy Clay Loam
71 - 80	Sandy Clay Loam							
81 - 90		Sandy Clay Loam			Sandy Clay Loam	Sandy Clay Loam	Sandy Clay Loam	
91 - 100				Sandy Clay Loam				
101 - 110	N/A							
111 - 120	Sandy Clay Loam	Sandy Clay Loam						Sandy Clay Loam
121 - 130								
131 - 140			Sandy Clay Loam		Sandy Clay Loam			
141 - 150								
151 - 160	Sandy Clay Loam	Sandy Clay Loam	Sandy Loam	Sandy Clay Loam	Sandy Clay Loam	Sandy Clay Loam	Sandy Clay Loam	Sandy Clay Loam
161 - 170								
171 - 180			Sandy Clay Loam					
181 - 190		Loam			Sandy Clay Loam	Sandy Clay Loam		
191 - 200							Sandy Clay Loam	
201 - 210								
211 - 220								
221 - 230								
231 - 240								Loam
241 - 250								
251 - 260								
261 - 270								
271 - 280								
281 - 290								Sandy Clay Loam
291 - 300								
301 - 305								

The chloride content within the field cores is listed and illustrated in Table 2 below. In general, it appears that more chloride can be found at greater depth and closer to the bottom of the ditch (location C) at both sites. The largest values were observed at the location nearest the edge of pavement (location A) at greater than 150 cm. This could be explained by consistent salt applications during the winter months followed by increased summer precipitation, which has been observed in recent years (StarTribune, 2019). This could wash salt deeper into the soil near the pavement and cause higher salt accumulation at the bottom of the ditch due to the ability of intense rainfalls (with more runoff) to carry salt into the ditch.

The smallest values of chloride are observed to be furthest from the pavement on the backslope (location D). There are three possible explanations for presence of road salt at this location: 1) salt could be thrown approximately 15 m directly to the backslope of the ditch from the roadway, 2) salt-laden runoff could pool in the ditch to a depth of approximately 1 m, or 3) salt-laden water could travel horizontally in the soil beyond the ditch into the soils beneath the backslope.

Table 2: Chloride content (mg/kg soil) for Site SB-1: Sandy Loam (left) and SB-2: Silt Loam (right). A = near the edge of the pavement, B = midslope between pavement and bottom of the ditch, C = in the bottom of the ditch, D = midslope on the side of the ditch furthest from the roadway. Color coding from small values (white) to large values (red).

Depth	Site SB-1: Highway 52 & 67th Street; Sandy Loam Soil type: 896 (Kingsley-Mahtomedi Complex)				Site SB-2: Highway 52 & 75th Street; Silt Loam Soil type: 344 (silt loam)			
(cm)	A	B	C	D	A	B	C	D
0 - 10	17.91	23.62	64.89	10.62	18.35	18.58	26.9	21.41
11 - 20								
21 - 30	11.32	17.6		7.57	40.2	16.78		9.14
31 - 40			72.47					
41 - 50				7.85	33.56	13.68	43.95	
51 - 60		20.01	60.51	11.2				8.87
61 - 70	10.31			10.79	12.59	46.9		
71 - 80								
81 - 90		18.14						
91 - 100		29.01						8.94
101 - 110	15.25							
111 - 120	34.24							
121 - 130								
131 - 140			44.84		21.43			
141 - 150								
151 - 160	111.2	27.98	33.56	20.78	65.65	54.33	52.98	12.32
161 - 170								
171 - 180		64.13	37.15		69.35	49.67		
181 - 190								
191 - 200							49.17	
201 - 210								
211 - 220								
221 - 230								10.66
231 - 240								
241 - 250								
251 - 260								
261 - 270								
271 - 280								
281 - 290								9.54
291 - 300								
301 - 305								

The Sodium Adsorption Ratio (SAR) in the field cores is listed and illustrated in Table 3. The largest values occur near the pavement at site SB-1 and at depths greater than 150 cm. Elevated values also exist in the bottom of the ditch at both sites. This coincides with the high values of chloride content (Table 2) and further supports the movement of sodium and chloride into the soil, likely mobilized by summer precipitation.

Table 3: Sodium Adsorption Ratio (SAR) for Site SB-1: Sandy Loam (left) and SB-2: Silt Loam (right). A = near the edge of the pavement, B = midslope between pavement and bottom of the ditch, C = in the bottom of the ditch, D = midslope on the side of the ditch furthest from the roadway.

Depth	Site SB-1: Highway 52 & 67th Street; Sandy Loam Soil type: 896 (Kingsley-Mahtomedi Complex)				Site SB-2: Highway 52 & 75th Street; Silt Loam Soil type: 344 (silt loam)			
(cm)	A	B	C	D	A	B	C	D
0 - 10	N/A	N/A	N/A	N/A	N/A	N/A	N/A	N/A
11 - 20								
21 - 30	9.09	5.15		N/A	N/A	2.17		0.26
31 - 40			N/A					
41 - 50				N/A		3.13	8.9	
51 - 60		5.9			N/A			0.26
61 - 70	9.26		7.71	N/A				
71 - 80				0.82	4.66	5.74		
81 - 90		N/A						
91 - 100								0.26
101 - 110	N/A	5.35						
111 - 120	15.28							
121 - 130			N/A					
131 - 140					5.29			
141 - 150								
151 - 160	27.44	5.35	4.51	1.08	5.59	N/A	2.87	0.3
161 - 170								
171 - 180		10.17	6.4		7.98	3.96		
181 - 190							2.87	
191 - 200								
201 - 210								
211 - 220								
221 - 230								
231 - 240								0.31
241 - 250								
251 - 260								
261 - 270								
271 - 280								
281 - 290								N/A
291 - 300								
301 - 305								

The saturation extract electrical conductivity (mmhos/cm) in the field cores is listed and illustrated in Table 4. The values represent the electrical conductivity of water within the soil pores. The largest

values occur at depths greater than 150 cm and near the edge of the pavement, which coincides with high values for chloride content (Table 2) and SAR (Table 3). This correlation is to be expected because salt within the soil is quickly dissolved in the presence of water and is highly conductive.

Table 4: Saturation Extract Electrical Conductivity (mmhos/cm) for Site SB-1: Sandy Loam (left) and SB-2: Silt Loam (right). A = near the edge of the pavement, B = midslope between pavement and bottom of the ditch, C = in the bottom of the ditch, D = midslope on the side of the ditch furthest from the roadway. Color coding from small values (white) to large values (red).

Depth	Site SB-1: Highway 52 & 67th Street; Sandy Loam Soil type: 896 (Kingsley-Mahtomedi Complex)				Site SB-2: Highway 52 & 75th Street; Silt Loam Soil type: 344 (silt loam)			
(cm)	A	B	C	D	A	B	C	D
0 - 10	N/A	N/A	N/A	N/A	N/A	N/A	N/A	N/A
11 - 20								
21 - 30	0.5	0.3		N/A	N/A	0.4		0.3
31 - 40			N/A				0.7	
41 - 50				N/A		0.4		
51 - 60		0.5			N/A			0.2
61 - 70	0.4		0.9	N/A				
71 - 80					0.4	0.6		
81 - 90		N/A		0.3				
91 - 100								
101 - 110	N/A	0.5						0.2
111 - 120	0.7							
121 - 130			N/A		0.5			
131 - 140								
141 - 150								
151 - 160	1.8	0.5	0.5	0.4	1.1	N/A	0.7	0.3
161 - 170								
171 - 180		0.9	0.7		1	0.6	0.6	
181 - 190								
191 - 200								
201 - 210								
211 - 220								
221 - 230								
231 - 240								
241 - 250								0.2
251 - 260								
261 - 270								
271 - 280								
281 - 290								N/A
291 - 300								
301 - 305								

The cation exchange capacity (meg/100g) in the field cores is listed and illustrated in Table 5. The values vary throughout the soil profile and between locations, but the largest values are present near the surface (shallow depth) furthest from the pavement and down in the bottom of the ditch (locations C

and D). Large values also appear at deeper depths (> 200 cm) at site SB-2. Smaller values indicate less potential for cation exchange and thus sodium (and chloride) may travel more readily. Larger values indicate more potential for cation exchange and thus sodium (and chloride) may be more likely to accumulate. High values of cation exchange capacity in the bottom of the ditch coincide with chloride content (Table 2), SAR (Table 3), and saturation extract electrical conductivity (Table 4).

Table 5: Cation Exchange Capacity (meq/100g) for Site SB-1: Sandy Loam (left) and SB-2: Silt Loam (right). A = near the edge of the pavement, B = midslope between pavement and bottom of the ditch, C = in the bottom of the ditch, D = midslope on the side of the ditch furthest from the roadway. Color coding from small values (white) to large values (red).

Depth	Site SB-1: Highway 52 & 67th Street; Sandy Loam Soil type: 896 (Kingsley-Mahtomedi Complex)				Site SB-2: Highway 52 & 75th Street; Silt Loam Soil type: 344 (silt loam)			
(cm)	A	B	C	D	A	B	C	D
0 - 10	6.72	6.25	7.96	8.38	7.59	9.5	9	11.45
11 - 20								
21 - 30	3.87	5.74		5.88	5.25	3.07		7.39
31 - 40			8.17					
41 - 50				3.21	5.24	3.5	7.67	
51 - 60		6	7.55	3.81				5.32
61 - 70	4.2			5.54	3.52	6.65		
71 - 80								
81 - 90		4.13						
91 - 100		4.09						6.12
101 - 110	4.2							
111 - 120	4.51							
121 - 130			3.22		2.93			
131 - 140								
141 - 150								
151 - 160	4.52	2.92	2.22	4.95	3.13	7.77	7.84	6.68
161 - 170								
171 - 180		6.41	5.83		6.47	8.11		
181 - 190								
191 - 200							9.27	
201 - 210								
211 - 220								
221 - 230								
231 - 240								
241 - 250								9.63
251 - 260								
261 - 270								
271 - 280								
281 - 290								5.54
291 - 300								
301 - 305								

Organic content as measured by loss on ignition in the field cores is listed and illustrated in Table 6. The largest values of organic content are present near the surface (shallow depth). The topsoil is expected to have a high organic content compared to sandy loam and silt loam subsoils, which is confirmed by these organic content values. For comparison, the organic content used in the column experiments was 10% organic matter by volume, which is approximately equivalent to 3% by weight. This coincides with the values in the topsoil measured in the field cores (1.8 – 2.5%).

Table 6: Organic matter by loss of ignition (%) for Site SB-1: Sandy Loam (left) and SB-2: Silt Loam (right). A = near the edge of the pavement, B = midslope between pavement and bottom of the ditch, C = in the bottom of the ditch, D = midslope on the side of the ditch furthest from the roadway. Color coding from small values (white) to large values (red).

Depth	Site SB-1: Highway 52 & 67th Street; Sandy Loam Soil type: 896 (Kingsley-Mahtomedi Complex)				Site SB-2: Highway 52 & 75th Street; Silt Loam Soil type: 344 (silt loam)			
(cm)	A	B	C	D	A	B	C	D
0 - 10	1.9	2.4	1.8	2.5	2.3	2.3	1.4	2.4
11 - 20								
21 - 30	0.3	1	0.6	1.1	0.5	0.5	0.8	0.8
31 - 40								
41 - 50				0.3	0.5	0.3		
51 - 60		0.6	0.7					0.4
61 - 70	0.2			0.3				
71 - 80				0.4	0.3	0.5		
81 - 90		0.2						
91 - 100								
101 - 110	0.4	0.2						0.4
111 - 120	0.2							
121 - 130								
131 - 140			0.2		0.2			
141 - 150								
151 - 160	0.2	0.6	0.2	0.3	0.2	1.5	0.9	0.7
161 - 170								
171 - 180		0.3	0.3		0.5	0.8	1.5	
181 - 190								
191 - 200								
201 - 210								
211 - 220								
221 - 230								
231 - 240								0.9
241 - 250								
251 - 260								
261 - 270								
271 - 280								
281 - 290								0.6
291 - 300								
301 - 305								

Total organic carbon (% C) is listed and illustrated in Table 7. The largest values occur in the bottom of the ditch (location C) at depths greater than 180 cm, though values in the topsoil were not measured. It is expected that if total organic carbon were measured for all segments, the values would coincide with organic matter (Table 6).

Table 7: Total organic carbon (% C) for Site SB-1: Sandy Loam (left) and SB-2: Silt Loam (right). A = near the edge of the pavement, B = midslope between pavement and bottom of the ditch, C = in the bottom of the ditch, D = midslope on the side of the ditch furthest from the roadway. Color coding from small values (white) to large values (red).

Depth	Site SB-1: Highway 52 & 67th Street; Sandy Loam Soil type: 896 (Kingsley-Mahtomedi Complex)				Site SB-2: Highway 52 & 75th Street; Silt Loam Soil type: 344 (silt loam)			
(cm)	A	B	C	D	A	B	C	D
0 - 10	N/A	N/A	N/A	N/A	N/A	N/A	N/A	N/A
11 - 20								
21 - 30	0.32	0.51		N/A	N/A	0.32		0.27
31 - 40			N/A				0.35	
41 - 50				N/A		0.22		
51 - 60		0.46		N/A	N/A			< 0.088
61 - 70			0.21			0.1		
71 - 80	0.24			0.36	0.26			
81 - 90		N/A						
91 - 100		0.15						0.14
101 - 110	N/A							
111 - 120	0.21							
121 - 130			N/A		0.13			
131 - 140								
141 - 150								
151 - 160	0.15	< 0.088	< 0.088	0.3	0.34		0.53	0.23
161 - 170								
171 - 180		0.84	0.37		0.2	0.25	0.83	
181 - 190								
191 - 200								
201 - 210								
211 - 220								
221 - 230								
231 - 240								
241 - 250								0.36
251 - 260								
261 - 270								
271 - 280								
281 - 290								
291 - 300								
301 - 305								

4.3 MODELING

Typical observed and simulated chloride breakthrough curves are given in Figure 18 and Figure 19.The data are plotted with depth on the x-axis, where depth is the cumulative water depth that has passed though the soil column. In all cases, better (lower RMSE) simulations of the observed breakthrough curves were obtained using the mobile-immobile solute transport model in Hydrus. The improvement in fit obtained with the mobile-immobile model is illustrated in Figure 18 for the sandy loam column with 10% organic. However, even for the same soil column, model parameters needed to be adjusted for each run (Table 8). In Figure 19, the two plots represent two subsequent runs in the same silt loam soil column, but the observed saturated hydraulic conductivity (Ksat) and calibrated soil porosity (θ) changed, with Ksat changing from 6.1 to 9.2 cm/hour, and θ changing from 0.38 to 0.46. This suggests that the soil column properties changed over the course of multiple runs, either due to shifting of the particles in soil column or due to the chloride loading (or both).

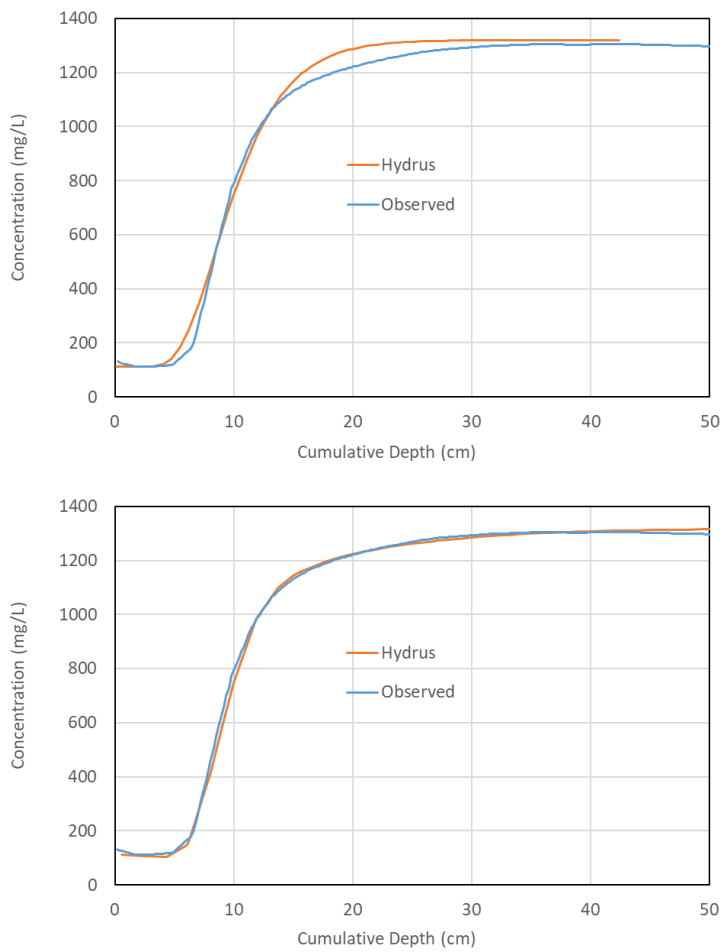

Figure 18: Simulated and observed chloride concentration vs. cumulative depth for column 5 with sandy loam + 10% organic matter. The upper panel gives the best-fit Hydrus simulation results for a linear model, while results in the lower panel include the mobile-immobile model with 8% immobile pores.

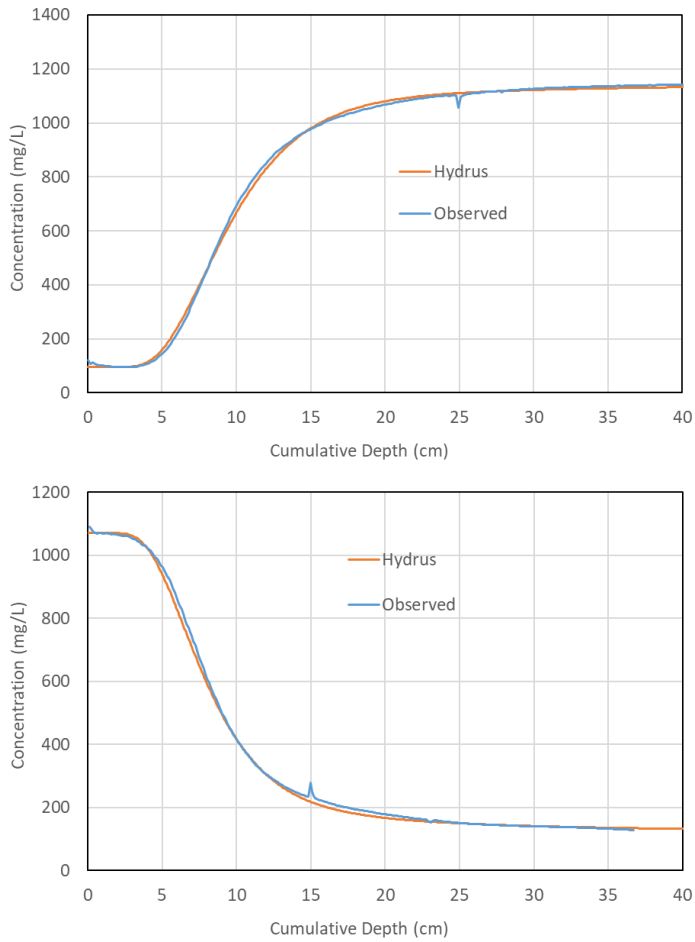

Figure 19: Simulated and observed chloride concentration vs. cumulative depth for silt loam columns during a chloride loading cycle (upper panel) and a subsequent flushing cycle (lower panel).

Some variability in the run-to-run calibrated porosities were obtained (Table 8), and some differences were observed between the calibrated porosities and the measured porosities at the completion of the experimental work. For the silt loam column, the average porosity calibrated from the Hydrus models (0.41) nearly matched average value of 0.40 measured in the soil columns. For the sandy loam and sandy loam with 10% organic, the modeled porosities were 0.37 and 0.40, respectively, while the measured values of 0.35 and 0.34, respectively.

Table 8: Summary of soil column runs modeled in Hydrus, and the key calibration parameters adjusted for each run. The 10-17 and 10-30 runs were flushing runs, while 10-23 and 11-5 were chloride loading runs.

Soil type	Experiment Phase	Ksat (cm/hr)	Total Porosity	Immobile Porosity	Dispersivity (cm)	Immobile pore rate constant (1/hour)
Sandy Loam (rep. 2)	Phase 2 salt-free rinse	20.7	0.37	0.10	7	0.04
	Phase 3 salt add	92.3	0.35	0.04	21	0.02
	Phase 3 salt-free rinse	29.1	0.40	0.06	5.5	0.30
Sandy Loam, 10% Org. (rep. 2)	Phase 2 salt-free rinse	28.2	0.35	0.04	1.8	0.1
	Phase 3 salt add	108.1	0.46	0.08	0.8	1.0
	Phase 3 salt-free rinse	27.3	0.39	0.10	0.2	0.4
Silt Loam (rep. 5)	Phase 2 salt-free rinse	6.1	0.39	0.06	2.3	0.02
	Phase 3 salt add	9.2	0.44	0.05	2.5	0.02
	Phase 3 salt-free rinse	3.0	0.40	0.035	2.0	0.015

CHAPTER 5: CONCLUSIONS

The purpose of this project was to measure the transport of chloride from road salt through soils commonly found in Minnesota. Previous research in Minnesota and other areas have shown that chloride does not always move freely with water but can interact with soil in unexplained ways. Involved processes appear to be anion exchange, temporary storage and subsequent release in organic compounds, and interactions with microorganisms, among others. Temperature and soil saturation levels may also impact the transport of chloride. The result is periods of chloride capture in soil and other periods of chloride release, which impacts chloride transport and can ultimately impact surface and groundwater resources.

This portion of the project used column experiments to illustrate chloride movement through three soils: silt loam, sandy loam, and sandy loam with 10% organic material which are common in Minnesota. The experiments totaled five phases of dosing with road salt followed by rinsing without road salt. The column experiments showed that chloride is sometimes stored within the soil and is released at other times. The trend approaching steady state was consistent with the three soils: Phase 1 dosing at 1000 mg/L resulted in the effluent approaching ~85% of the influent, indicating that ~15% of the salt dosing was not leaving the columns. Phase 2 dosing with 640 mg/L resulted in the effluent approaching the influent concentration, indicating that there were remnants of the phase 1 dosing leaving the soil columns. Phase 2 dosing with 1000 mg/L resulted in the effluent exceeding the influent concentration, indicating that the stored material had been adsorbed and was now released into the column effluent. Phase 3 dosing at 1400 mg/L resulted in the effluent approaching ~85% of the influent increased concentration. Phases 4 and 5 dosing at 1000 mg/L resulted in an effluent concentration that was higher than the influent concentration, which could be interpreted as a continued release of the chloride that was stored during Phase 3. It is unclear from these experiments what factors control chloride capture and release. Storage in capillary spaces in the soil could explain the results of phases 1, 4 and 5, but the result of Phase 2 indicates that adsorption of chloride is taking place. This explanation is contrary to the accepted process for chloride movement and fate in soils and needs to be investigated further.

Field cores were also collected at two sites targeting silt loam and sandy loam, though texture analysis revealed that the cores were primarily sandy clay loam with portions of silt loam and sandy loam. The results of the field cores demonstrate that chloride is present in the soil along roadways that are treated with deicing road salt. Sodium adsorption ratio and saturation extract electrical conductivity coincided with chloride content, which is expected. Other properties such as cation exchange capacity, organic content, and soil texture did not consistently correlate with chloride content and thus cannot be used to predict chloride presence or transport.

Although it is not clear from the column experiments or field cores which soil or hydraulic properties cause capture or release of chloride from road salt, the data demonstrate that chloride is stored within the soil, requiring a long period of freshwater rinse (tens to hundreds of years) before it can leave, and that chloride in our groundwater will be a legacy for some time even after alternative solutions to chloride-based salts have been established and accepted.

CHAPTER 6: REFERENCES

Albright, W. H., Benson, C. H., Gee, G. W., Roesler, A. C., Abichou, T., Apiwantragoon, P., . . . Rock, S. A. (2004). Field water balance of landfill final covers. *Journal of Environmental Quality, 33*(6), 2317-2332. doi:10.2134/jeq2004.2317

aqion. (2019). Temperature Compensation for Conductivity. Retrieved from https://www.aqion.de/site/112

Bastviken, D., Sanden, P., Svensson, T., Stahlberg, C., Magounakis, M., & Oberg, G. (2006). Chloride-retention and release in a boreal forest soil: Effects of soil water residence time and nitrogen and chloride loads. *Environmental Science & Technology, 40*(9), 2977-2982. doi:10.1021/es0523237

Bastviken, D., Svensson, T., Karlsson, S., Sandén, P., & Öberg, G. (2009). Temperature Sensitivity Indicates That Chlorination of Organic Matter in Forest Soil Is Primarily Biotic. doi:10.1021/es8035779

Bastviken, D., Thomsen, F., Svensson, T., Karlsson, S., Sanden, P., Shaw, G., . . . Oberg, G. (2007). Chloride retention in forest soil by microbial uptake and by natural chlorination of organic matter. *Geochimica Et Cosmochimica Acta, 71*(13), 3182-3192. doi:10.1016/j.gca.2007.04.028

Bejat, L., Perfect, E., Quisenberry, V. L., Coyne, M. S., & Haszler, G. R. (2000). Solute transport as related to soil structure in unsaturated intact soil blocks. *Soil Science Society of America Journal, 64*(3), 818-826. doi:10.2136/sssaj2000.643818x

Biester, H., Keppler, F., Putschew, A., Martinez-Cortizas, A., & Petri, M. (2004). Halogen retention, organohalogens, and the role of organic matter decomposition on halogen enrichment in two Chilean peat bogs. *Environmental Science & Technology, 38*(7), 1984-1991. doi:10.1021/es0348492

Clarke, N., Fuksova, K., Gryndler, M., Lachmanova, Z., Liste, H. H., Rohlenova, J., . . . Matucha, M. (2009). The formation and fate of chlorinated organic substances in temperate and boreal forest soils. *Environmental Science and Pollution Research, 16*(2), 127-143. doi:10.1007/s11356-008-0090-4

Cooper, C. A., Mayer, P. M., & Faulkner, B. R. (2014). Effects of road salts on groundwater and surface water dynamics of sodium and chloride in an urban restored stream. *Biogeochemistry, 121*(1), 149-166. doi:10.1007/s10533-014-9968-z

Fetisova, N. F., Fetisov, V. V., De Maio, M., & Zektser, I. S. (2016). Groundwater vulnerability assessment based on calculation of chloride travel time through the unsaturated zone on the area of the Upper Kama potassium salt deposit. *Environmental Earth Sciences, 75*(8). doi:10.1007/s12665-016-5496-6

Gryndler, M., Rohlenova, J., Kopecky, J., & Matucha, M. (2008). Chloride concentration affects soil microbial community. *Chemosphere, 71*(7), 1401-1408. doi:10.1016/j.chemosphere.2007.11.003

Gustavsson, M., Karlsson, S., Oberg, G., Sanden, P., Svensson, T., Valinia, S., . . . Bastviken, D. (2012). Organic Matter Chlorination Rates in Different Boreal Soils: The Role of Soil Organic Matter Content. *Environmental Science & Technology, 46*(3), 1504-1510. doi:10.1021/es203191r

Hazlehurst, T. H., Martin, H. C., & Brewer, L. (1936). The creeping of saturated salt solutions. *Journal of Physical Chemistry, 40*(4), 439-452. doi:10.1021/j150373a003

Heitkamp, B., & Marr, J. (2015). *Minnesota Steel Culvert Pipe Service-Life Map*. Retrieved from https://conservancy.umn.edu/handle/11299/174177

Hu, Y., Zhang, C., Wang, D. Z., Wen, J. Y., Chen, M. H., & Li, Y. (2013). Chloride ion transport and fate in oilfield wastewater reuse by interval dynamic multimedia aquivalence model. *Water Science and Technology, 67*(3), 628-634. doi:10.2166/wst.2012.609

Jin, L., Whitehead, P., Siegel, D. I., & Findlay, S. (2011). Salting our landscape: An integrated catchment model using readily accessible data to assess emerging road salt contamination to streams. *Environmental Pollution, 159*(5), 1257-1265. doi:10.1016/j.envpol.2011.01.029

Johansson, E., Sanden, P., & Oberg, G. (2003). Spatial patterns of organic chlorine and chloride in Swedish forest soil. *Chemosphere, 52*(2), 391-397. doi:10.1016/s0045-6535(03)00193-0

Kelly, V. R., Lovett, G. M., Weathers, K. C., Findlay, S. E. G., Strayer, D. L., Burns, D. J., & Likens, G. E. (2008). Long-term sodium chloride retention in a rural watershed: Legacy effects of road salt on streamater concentration. *Environmental Science & Technology, 42*(2), 410-415. doi:10.1021/es071391l

Kincaid, D. W., & Findlay, S. E. G. (2009). Sources of Elevated Chloride in Local Streams: Groundwater and Soils as Potential Reservoirs. *Water Air and Soil Pollution, 203*(1-4), 335-342. doi:10.1007/s11270-009-0016-x

Kinjo, T., & Pratt, P. F. (1971). Nitrate Adsorption: II. In Competition with Chloride, Sulfate, and Phosphate 1. doi:10.2136/sssaj1971.03615995003500050028x

Kopacek, J., Hejzlar, J., Porcal, P., & Posch, M. (2014). A mass-balance study on chloride fluxes in a large central European catchment during 1900-2010. *Biogeochemistry, 120*(1-3), 319-335. doi:10.1007/s10533-014-0002-2

Krzmarzick, M. J., Crary, B. B., Harding, J. J., Oyerinde, O. O., Leri, A. C., Myneni, S. C. B., & Novak, P. J. (2012). Natural Niche for Organohalide-Respiring Chloroflexi. *Applied and Environmental Microbiology, 78*(2), 393-401. doi:10.1128/aem.06510-11

Krzmarzick, M. J., McNamara, P. J., Crary, B. B., & Novak, P. J. (2013). Abundance and diversity of organohalide-respiring bacteria in lake sediments across a geographical sulfur gradient. *Fems Microbiology Ecology, 84*(2), 248-258. doi:10.1111/1574-6941.12059

Lax, S., & Peterson, E. W. (2009). Characterization of chloride transport in the unsaturated zone near salted road. *Environmental Geology, 58*(5), 1041-1049. doi:10.1007/s00254-008-1584-6

Leri, A. C., & Myneni, S. C. B. (2010). Organochlorine turnover in forest ecosystems: The missing link in the terrestrial chlorine cycle. *Global Biogeochemical Cycles, 24*. doi:10.1029/2010gb003882

MnDOT. (2019). Maintaining Minnesota's Highways. Retrieved from https://www.dot.state.mn.us/maintenance/faq.html

Montelius, M., Thiry, Y., Marang, L., Ranger, J., Cornelis, J. T., Svensson, T., & Bastviken, D. (2015). Experimental Evidence of Large Changes in Terrestrial Chlorine Cycling Following Altered Tree Species Composition. *Environmental Science & Technology, 49*(8), 4921-4928. doi:10.1021/acs.est.5b00137

MPCA. (2019). Statewide Chloride Management Plan. Retrieved from https://www.pca.state.mn.us/sites/default/files/wq-s1-94.pdf

Myneni, S. C. B. (2002). Formation of stable chlorinated hydrocarbons in weathering plant material. *Science, 295*(5557), 1039-1041. doi:10.1126/science.1067153

Norouzi Rad, M., & Shokri, N. (2015). Effects of texture on salt precipitation dynamics and deposition patterns in drying porous media. *EGUGA*, 12200.

Novotny, E. V., Murphy, D., & Stefan, H. G. (2008). Increase of urban lake salinity by road deicing salt. *Science of The Total Environment, 406*(1-2), 144.

Oberg, G., Holm, M., Sanden, P., Svensson, T., & Parikka, M. (2005). The role of organic-matter-bound chlorine in the chlorine cycle: a case study of the Stubbetorp catchment, Sweden. *Biogeochemistry, 75*(2), 241-269. doi:10.1007/s10533-004-7259-9

Oberg, G., & Sanden, P. (2005). Retention of chloride in soil and cycling of organic matter-bound chlorine. *Hydrological Processes, 19*(11), 2123-2136. doi:10.1002/hyp.5680

Sghaier, N., Prat, M., & Ben Nasrallah, S. (2006). On the influence of sodium chloride concentration on equilibrium contact angle. *Chemical Engineering Journal, 122*(1-2), 47-53. doi:10.1016/j.cej.2006.02.017

Simunek, J., van Genuchten, M. T., & Sejna, M. (2016). Recent Developments and Applications of the HYDRUS Computer Software Packages. *Vadose Zone Journal, 15*(7). doi:10.2136/vzj2016.04.0033

StarTribune. (2019, October 3, 2019). Rain on top of rain makes Minnesota one wet mess. Retrieved from http://www.startribune.com/enough-already-rain-rain-go-away/562025112/

Svensson, T., Lovett, G. M., & Likens, G. E. (2012). Is chloride a conservative ion in forest ecosystems? *Biogeochemistry, 107*(1-3), 125-134. doi:10.1007/s10533-010-9538-y

Svensson, T., Sanden, P., Bastviken, D., & Oberg, G. (2007). Chlorine transport in a small catchment in southeast Sweden during two years. *Biogeochemistry, 82*(2), 181-199. doi:10.1007/s10533-006-9062-2

van Genuchten, M. T. (1980). A Closed-form Equation for Predicting the Hydraulic Conductivity of Unsaturated Soils. *Soil Science Society of America Journal, 44*(5), 892-898. doi:10.2136/sssaj1980.03615995004400050002x

Washburn, E. R. (1927). The Creeping of Solutions. *Journal of Physical Chemistry*. doi:10.1021/j150278a009

Zhang, Z., Hu, H. C., Tian, F. Q., Hu, H. P., Yao, X. H., & Zhong, R. S. (2014). Soil salt distribution under mulched drip irrigation in an arid area of northwestern China. *Journal of Arid Environments, 104*, 23-33. doi:10.1016/j.jaridenv.2014.01.012